

Coxiella burnetii modulates Beclin 1 and Bcl-2, preventing host cell apoptosis to generate a persistent bacterial infection

CL Vázquez¹ and MI Colombo^{*1}

Coxiella burnetii is the etiological agent of the human disease, Q fever, and is an obligate intracellular bacterium that invades and multiplies in a vacuole with lysosomal characteristics. We have previously shown that *Coxiella* interacts with the autophagic pathway as a strategy for its survival and replication. In addition, recent studies have shown that *Coxiella* exerts anti-apoptotic activity to maintain the host cell viability, thus generating a persistent infection. In the present report, we have explored the role of Beclin 1 and Bcl-2 in *C. burnetii* infection to elucidate how this bacterium modulates autophagy and apoptosis to its own benefit. Beclin 1, a Bcl-2 interacting protein, is required for autophagy. In this study, we show that Beclin 1 is recruited to the *Coxiella*-membrane vacuole, favoring its development and bacterial replication. In contrast, the anti-apoptotic protein Bcl-2 alters the normal development of the *Coxiella*-replicative compartment, in spite of also being recruited to the vacuole membrane. Furthermore, both vacuole development and the anti-apoptotic effect of *C. burnetii* are affected by Beclin 1 depletion and by the expression of a Beclin 1 mutant defective in Bcl-2 binding. Overall, these findings indicate that *C. burnetii* infection modulates autophagy and apoptotic pathways through Beclin 1/Bcl-2 interplay to establish a successful infection in the host cell.

Cell Death and Differentiation (2010) 17, 421–438; doi:10.1038/cdd.2009.129; published online 2 October 2009

The macroautophagy pathway (hereafter, autophagy) is a physiological process, ubiquitous in eukaryotic cells. It is involved in the sequestration of cytoplasm or damaged organelles in double-membrane vesicles called autophagosomes. Subsequently, these vesicles fuse with late endosomes and lysosomes, which supply the hydrolytic enzymes, to generate the autolysosomes, in which the sequestered material is degraded.^{1,2} Autophagy can be stimulated in response to cell stress, such as nutrient deprivation and pathogen invasion, or it may occur at a basal level operating as a cell quality control mechanism to eliminate aged organelles and unnecessary structures.³ Many Atg proteins (i.e. autophagy related) function during the different stages of autophagosome biogenesis.⁴ The early events in the autophagy pathway involve the complex formed by Atg6 (orthologous to mammalian Beclin 1), Atg14, Vps15 and the class III PI-3 kinase (hVps34), which are essential for the recruitment of other Atg proteins to the isolation membrane or phagophore (autophagosome precursors).^{5–7} Two ubiquitin-like modification systems, the Atg12–Atg5 complex and the Atg8 (also known as LC3), act in autophagosome formation.⁸ Initially, Atg12 is activated and conjugated to Atg5 to localize at the isolation membrane. Then, the Atg12–Atg5 complex is dissociated with the completion of the autophagic vesicle formation,^{9–11} for which the LC3 protein is also required. LC3 exists in two forms: the cytosolic form (LC3-I) and the lipidated

form (LC3-II) targeted to the autophagosomal membrane. LC3 remains associated, at least in part, even after fusion with lysosomes, when LC3-II is delipidated and recycled back to the cytoplasm.^{12,13}

The gene *Beclin 1* is a haploinsufficient tumor suppressor in mice^{14,15} and the human gene is monoallelically deleted in several cancers.¹⁶ Initially, Beclin 1 was identified as a Bcl-2 interacting protein¹⁷ and has been implicated as an important regulator of autophagy. The suppression of Beclin 1 expression impairs autophagy and sensitizes the cells to starvation-induced apoptosis.¹⁸ Beclin 1 has a BH3 domain by which it interacts with proteins of the Bcl-2 family, including Bcl-2 and Bcl-X_L, both of which are inhibitors of apoptosis.^{19,20} It has been shown that the interaction between Bcl-2 and Beclin 1 leads to inhibition of autophagy by interfering with the formation and activity of the autophagy promoter complex, Beclin 1/hVps34.²¹

Multiple intracellular pathogens, such as *Porphyromonas gingivalis*,²² *Brucella abortus*²³ and *Legionella pneumophila*,²⁴ use the autophagy pathway to their own benefit. *Coxiella burnetii* (hereafter *Cb*) is a gram-negative bacterium that causes the Q fever in humans. It has a biphasic life cycle, involving the infectious particles (small cell variant (SCV)) and the metabolic and replicative active form (large cell variant (LCV)).^{25,26} In addition, *Cb* presents a type IV secretion system (T4SS) that injects bacterial effectors into host cells.

¹Laboratorio de Biología Celular y Molecular- Instituto de Histología y Embriología (IHEM), Facultad de Ciencias Médicas, Universidad Nacional de Cuyo-CONICET, Mendoza, Argentina

*Corresponding author: MI Colombo, Laboratorio de Biología Celular y Molecular, Instituto de Histología y Embriología (IHEM)-CONICET, Facultad de Ciencias Médicas, Universidad Nacional de Cuyo, Casilla de Correo 56, Centro Universitario, Parque General San Martín, (5500) Mendoza 5500, Argentina. Tel: +54 261 4494143 Ext. 2690; Fax: +54 261 4494117; E-mail: mcolombo@fcm.uncu.edu.ar

Keywords: Beclin 1; Bcl-2; apoptosis; autophagy

Abbreviations: *Cb*, *Coxiella burnetii*; CRV, *Coxiella*-replicative vacuoles; T4SS, type IV secretion system

Received 12.12.08; revised 16.7.09; accepted 09.8.09; Edited by V De Laurenzi; published online 02.10.09

These bacterial molecules likely orchestrate host cell processes, allowing the establishment of a productive infection and intracellular survival of this microorganism.²⁷ Our group has shown that *Cb* survives and replicates in a large replicative vacuole (*C. burnetii*-replicative vacuoles (CRVs)) with clear autophagic features.²⁸ Besides, autophagy induction before infection, as well as the overexpression of proteins involved in this pathway (i.e. LC3 and Rab24), favors the development of the CRV at early post-infection (p.i.) times.²⁹ Moreover, we have shown that *Cb* invades host cells through a classical phagocytosis involving normal components of the endocytic/phagocytic pathway. In addition, this pathogen actively interacts with autophagosomes to delay the arrival of hydrolytic enzymes facilitating vacuole development.³⁰ The generation and maturation of the large CRV require a sustained bacterial protein synthesis.³¹

Cb has the ability to induce persistent infections in host cells;^{32,33} therefore, recent studies have been designed to understand the strategies that *Cb* uses to control the fate of the host cell. It has been shown that *Cb* infection inhibits apoptosis in host cells, allowing bacterial survival and multiplication.^{34,35} One of the proposed mechanisms by which *Cb* exerts its anti-apoptotic effect is by preventing the release of cytochrome *c*, thus avoiding the activation of executioner caspases.³⁵ Besides, a recent study has shown that *Cb* infection modulates the expression of apoptosis-related genes.³⁴

In view of these results, an interesting point to analyze is how *Cb* modulates both autophagy and apoptosis, two pathways that are intimately associated, to develop a successful infection. In this study, we show that *Cb* recruits Beclin 1 to the CRV and that the development of this vacuole is favored by the overexpressed Beclin 1. In contrast, overexpressed Bcl-2 alters the development of the normal CRV, in spite of also being recruited to the vacuole membrane. We propose that *Cb* modulates the interplay between Beclin 1 and Bcl-2 to exert its anti-apoptotic activity.

Results

Beclin 1 decorates CRVs and favors its development. At 48 h p.i., *Cb* develops a large CRV that presents the features of a phagolysosomal vacuole.^{25,32} To examine the role of Beclin 1 in *Cb* infection, cells were infected with *Cb* for 48 h and both the bacterium and Beclin 1 were detected. Interestingly, we observed the accumulation of endogenous

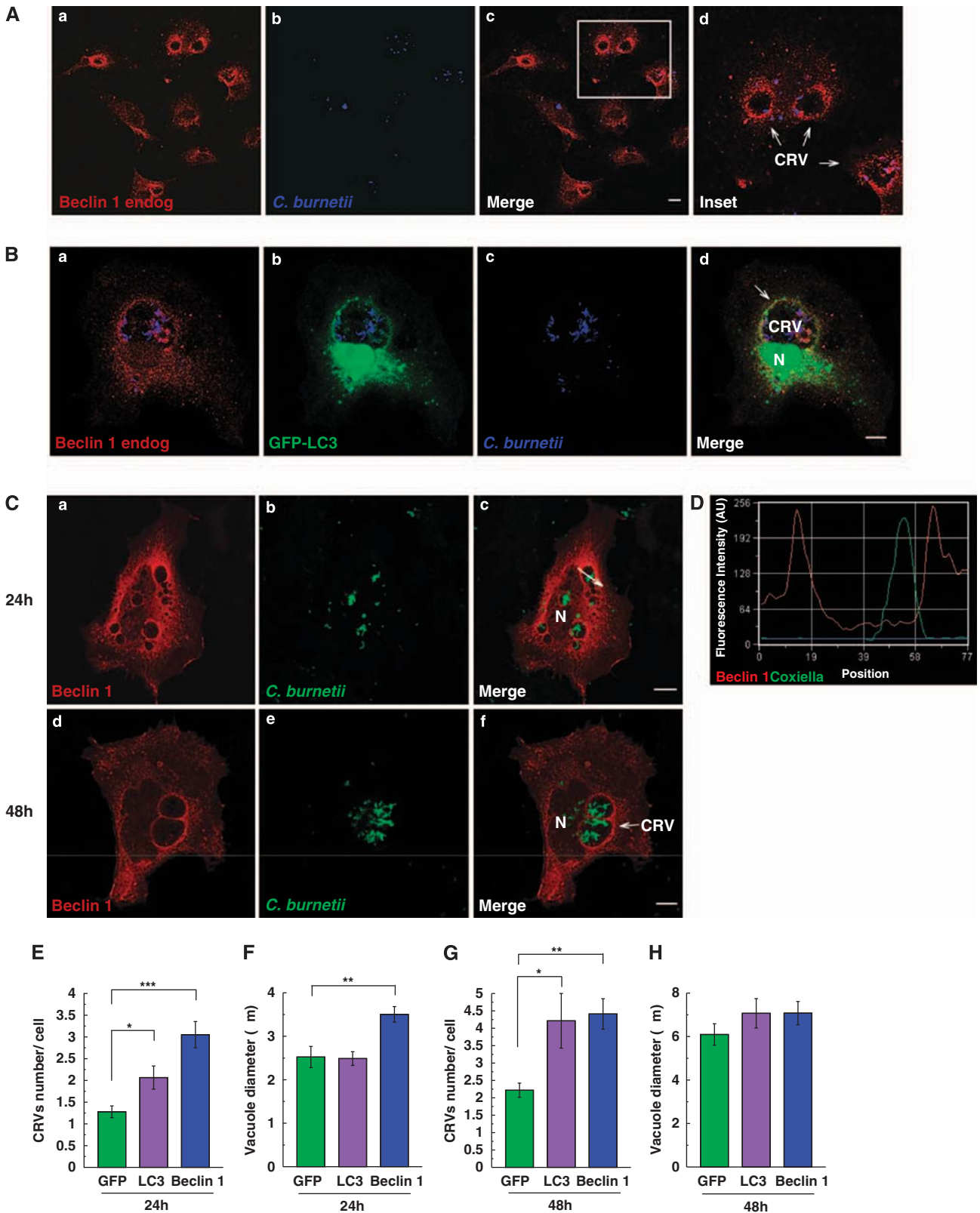
Beclin 1 in the surrounding membrane of the CRV (Figure 1A). We have previously shown that LC3 also associates with the large CRV;²⁹ therefore, we next examined whether both Beclin 1 and LC3 were recruited to the same vacuole. Figure 1B clearly shows both endogenous Beclin 1 and GFP-LC3 decorating the large CRV. To examine in detail the distribution and function of Beclin 1 in *Cb* infection, we overexpressed this protein in HeLa cells. After a transient transfection with FLAG-Beclin 1, cells were infected with *Cb* for 24 or 48 h (Figure 1C). At 24 h p.i., panels a–c show several CRVs decorated with Beclin 1, and by 48 h (panels d–f) two typical large CRVs, also decorated by Beclin 1, are depicted, which probably were formed by the fusion of smaller ones. Figure 1D shows the quantification of the fluorescence intensity along the white arrow across the CRV depicted in Figure 1C, panel c. The graph shows the accumulation of Beclin 1 (red) at the surrounding CRV membrane.

We next assessed whether CRV development was affected by the overexpression of Beclin 1, by determining the parameters related to *Cb* infection, such as the number of infected cells, vacuole size and number of CRVs per cell. No differences were observed in the percentage of infected cells (cells that contain at least one intracellular bacterium) at 24 and 48 h in cells overexpressing Beclin 1, GFP-LC3 or GFP alone as a control (data not shown). However, at 6 h a significant increase was observed in the number of infected cells overexpressing Beclin 1 as well as GFP-LC3 compared with GFP (Supplementary Figure 1a). In contrast, by 12 h p.i. these differences were lost. Therefore, the overexpression of these proteins benefits the infection at earlier times, suggesting that the entry of the bacterium to transfected cells could be enhanced. In addition, we found a marked increase in the CRV number in cells overexpressing either LC3 or Beclin 1, both at 24 and 48 h, compared with cells overexpressing the vector GFP alone (Figures 1E and G). At 24 h, the diameter of CRVs in cells overexpressing Beclin 1 was also increased (Figure 1F). However, by 48 h the CRV diameter was similar in all cases (Figure 1H), indicating again that at later infection times these differences were lost. When the vacuole diameter data at 24 and 48 h were arranged in groups according to vacuoles size (Supplementary Figures 1b and c, respectively), we observed that in cells overexpressing Beclin 1 the amount of larger vacuoles was increased. These results indicate that, similar to LC3, overexpressed Beclin 1 favors CRV development at early times after infection, and confirm that the compartment in which *Cb* resides is targeted by autophagic proteins.

Figure 1 Beclin 1 decorates the CRV membrane and favors vacuole development. (A) HeLa cells were infected with *Cb* for 48 h, fixed and subjected to indirect immunofluorescence using an antibody against Beclin 1 to detect the endogenous protein (red, panel a), and anti-*Coxiella* to detect the bacterium (blue, panel b). The inset is shown in panel d. Cells were analyzed using confocal microscopy. The CRVs are indicated with white arrows. Scale bar: 10 μ m. (B) Endogenous Beclin 1 decorates the *Cb* membrane vacuole in cells transfected with GFP-LC3. Cells transfected with GFP-LC3 (panel b) were infected with *Cb* for 48 h, fixed and subjected to indirect immunofluorescence using an antibody against Beclin 1 to detect the endogenous protein (red, panel a) and anti-*Coxiella* (blue, panel c). The arrows show a CRV. N, nucleus. Scale bars: 10 μ m. (C) HeLa cells were transiently transfected with FLAG epitope-tagged human Beclin 1 and then infected. At 24 h (panels a–c) and 48 h p.i. (panels d–f), cells were fixed, subjected to immunofluorescence using a primary antibody against *Cb* (green, panels b and e) followed by a secondary antibody conjugated to Alexa 488. Beclin 1 was visualized with a mouse anti-FLAG (red, panels a and d) and incubated with the appropriate secondary antibody conjugated to Cy3. The white arrows indicate the CRVs. N, nucleus. Scale bars: 10 μ m. (D) shows the quantification of the fluorescence intensity along the white arrow in panel c, in (C). The white arrow in the merged image indicates the position and the direction of the profile line used for analysis. (E, G) The percentage of CRVs number per cell at 24 (E) and 48 h (G) in cells transfected with the control vector (GFP), GFP-LC3 or FLAG-Beclin 1 is shown. (F, H) The quantification of vacuole size (μ m) at 24 (F) and 48 h p.i. (H). The data in (E–H) represent the mean \pm S.E.M. of at least three independent experiments (number of counted cells = 100). Significantly different from control: * P < 0.05; ** P < 0.01; *** P < 0.001

The complex Beclin 1/hVps34 is recruited to the CRVs. We next analyzed the distribution and activity of the Beclin 1/hVps34 complex, using GFP-2xFYVE, a probe that

labels PI3P, the PI-3 kinase product (Figure 2A). Our findings indicated that from early p.i. times, both Beclin 1 and GFP-FYVE were decorating the limiting membrane of small



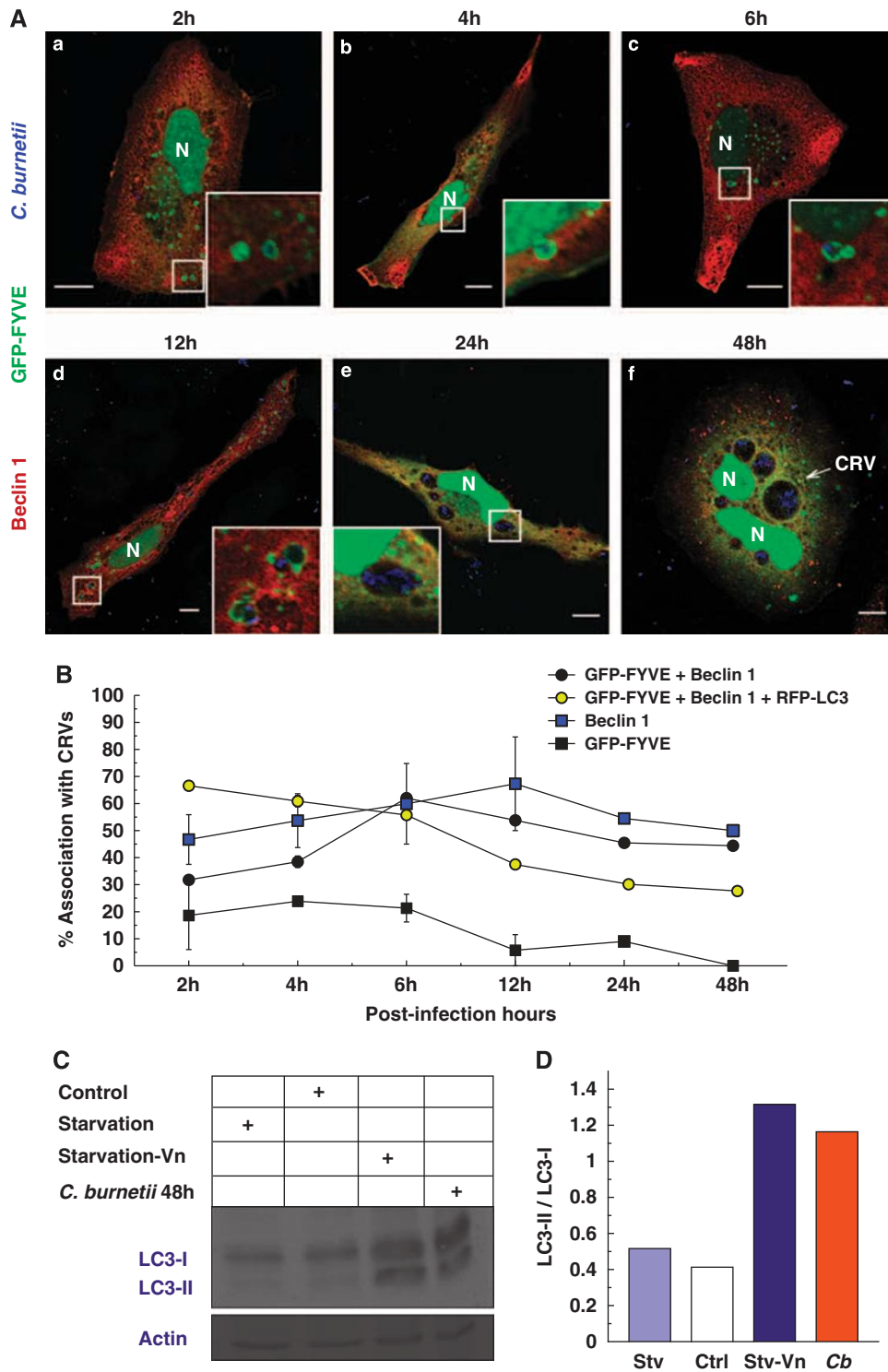


Figure 2 *C. burnetii* infection induces autophagy and the recruitment of an active Beclin 1/hVps34 complex to the CRV membrane. (A) HeLa cells transiently co-transfected with FLAG-Beclin 1 and GFP-2xFYVE were infected with *Cb* for different times (panels a–f). The cells were fixed and processed to detect Beclin 1 and the bacterium using specific antibodies (Beclin 1 in red and *Cb* in blue). GFP-2xFYVE is depicted in green. The images were captured using a confocal microscope. The insets show small CRVs at early p.i. times with both Beclin 1 and GFP-FYVE recruited to the vacuole membranes. N, nucleus. Scale bars: 10 μ m. (B) Quantification of the percentage of CRVs associated with Beclin 1 (blue squares), GFP-2xFYVE (closed squares), Beclin 1 and GFP-2xFYVE (closed circles) or triple-labeled GFP-2xFYVE, Beclin 1 and RFP-LC3 (yellow circles). The number of CRVs associated with both Beclin 1 and FYVE increased with the infection time. The data represent the mean \pm S.E.M. of at least three independent experiments (number of counted cells = 50). (C) HeLa cells were infected with *Cb* for 48 h and the LC3 conversion using western blot analysis was determined. The level of LC3 conversion in infected cells was compared with the uninfected cells incubated for 2 h in full nutrient media (control) or subjected to starvation in the absence (Stv) or presence of 100 μ M vinblastine (Vn). (D) Determination of LC3-II/ LC3-I ratio from the western blot is shown in (C)

vacuoles (insets in panels a–d) and even the large CRVs generated at 24 and 48 h (panels e and f). GFP-FYVE was also found in small vesicles dispersed throughout the cytoplasm, which likely represent early endosomes/autophagosomes. In addition, the percentage of CRVs associated with both Beclin 1 and FYVE increased with the infection time, being maximal at 6 h (Figure 2B), and were clearly present even at 48 h. These results show that Beclin 1 colocalizes with the active product of the PI-3 kinase, suggesting an active engagement of this kinase during *Cb* infection even after prolonged times of infection. Furthermore, when the triple colocalization among Beclin 1, the FYVE domain and RFP-LC3 was analyzed, the association of the markers was maintained at all p.i. times analyzed, corroborating that the relationship between Beclin 1 and the FYVE domain was indicative of a functional autophagic activity at the CRV.

To further corroborate that autophagy was indeed induced by *Cb* infection, we analyzed the processing of LC3 using western blot. As shown in Figure 2C, upon infection with this bacterium, a marked increase in the LC3-II form was observed, confirming the autophagy induction.

Suppression of Beclin 1 affects the normal CRV development. To determine whether Beclin 1 is actually required for the normal development of the CRVs, we analyzed whether a decrease in Beclin 1 expression had an effect on *Cb* infection. We used a plasmid encoding a small interference RNA against Beclin 1 (pSuper Beclin 1-KD, referred to as Beclin 1-KD), which causes the knockdown of transfected cells after 48 h. Cells were first infected with *Cb*, then they were transfected with the indicated plasmids (see the diagram in Figure 3A) and incubated for 48 h to diminish Beclin 1 levels. The expression levels of Beclin 1 in individual cells were detected with a specific antibody. As expected, in control cells (Figure 3B, panels a–c), endogenous Beclin 1 was recruited to the CRVs. However, in cells transfected with Beclin 1-KD, a very low detection of endogenous Beclin 1 was observed (panels d–f), corroborating the suppression of the protein expression. The number of CRVs in the co-transfected cells with Beclin 1-KD and GFP decreased when compared with cells overexpressing Beclin 1, but not with the control GFP (Figure 3C). However, we observed a significant decrease in vacuole size in cells transfected with Beclin 1-KD versus the control GFP (Figure 3D). These results suggest that Beclin 1 suppression disturbs the establishment of a normal CRV.

The no alterations in vesicle size observed in Figure 3C (comparing Beclin 1-KD with the control GFP) may be a consequence of a partial depletion in the endogenous Beclin 1 protein. Therefore, to achieve a more efficient knockdown of the protein, we used a different experimental strategy. Cells were first transfected twice (double-hit protocol) with the Beclin 1-KD plasmid before *Cb* infection (see Materials and Methods and the diagram in Figure 3E). Using western blot analysis, we confirmed that double transfection with the Beclin 1-KD plasmid resulted in the knockdown of Beclin 1 (Figure 3F), and that this double-hit protocol was more efficient in depleting endogenous Beclin 1 than the simple

one (not shown). For the last 24 h, cells were infected with *Cb*. Figure 3G shows infected cells overexpressing GFP (control) or Beclin 1-KD and GFP, wherein Beclin 1 was detected with a specific antibody. In the control cells, Beclin 1 was recruited to the small CRVs (panels a–c, white arrows). As expected, cells overexpressing Beclin 1-KD (cell marked with an asterisk, panels d–f), showed a low detection of the endogenous protein. With this experimental approach, we observed a significant decrease in both the number of CRVs and vacuole diameter in cells co-transfected with Beclin 1-KD and GFP (Figures 3H and I).

Previously published work indicates that the knockdown of Beclin 1 leads to autophagy inhibition.²¹ Therefore, in order to address whether Beclin 1 depletion also inhibited autophagy in our system, cells were subjected to the double-hit protocol, but were co-transfected with GFP-LC3 to analyze the number of autophagosomes. Cells were subsequently incubated in full nutrient media (Ctrl) or under starvation conditions (Stv) to induce autophagy. As shown in Figure 3J, the number of GFP-LC3-positive dots was significantly reduced in Beclin 1-KD-overexpressing cells.

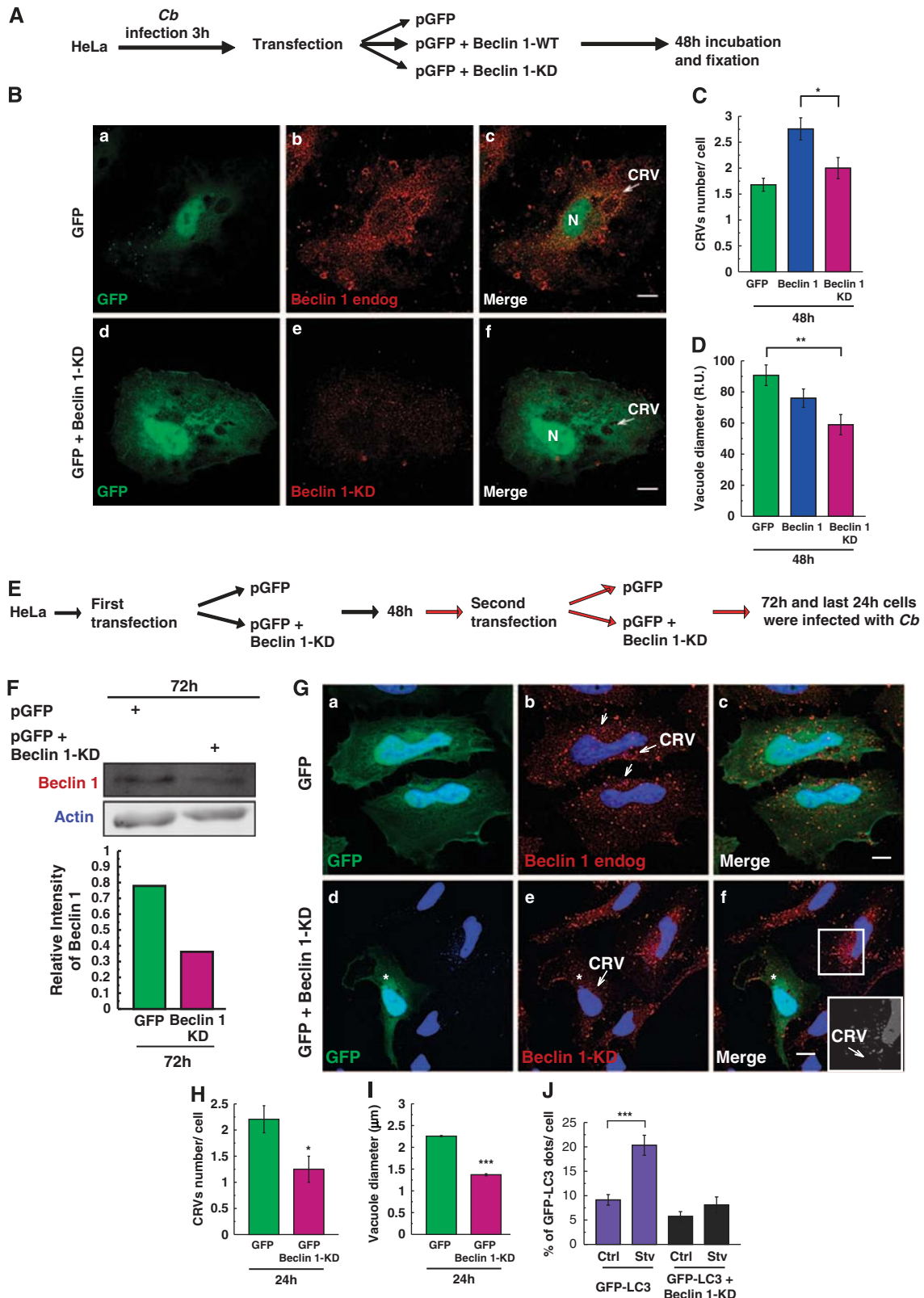
The beneficial effect of Beclin 1 in CRV development is not exerted by a Beclin 1 mutant unable to interact with Bcl-2. Previous studies have shown that Beclin 1 interacts with the anti-apoptotic protein Bcl-2 and this interaction is important for autophagy regulation.²¹ Therefore, we next explored whether the infection with *Cb* was affected by the overexpression of a mutant of Beclin 1 (Beclin 1-BD), which is defective in Bcl-2 binding.²¹ Figure 4A (panels a–c) shows Beclin 1-WT decorating the CRV membrane. In cells overexpressing Beclin 1-BD (panels d–f), the protein was also recruited to the CRVs. A quantitative analysis of the number of CRVs per cell and vacuole diameter showed a significant reduction in both parameters, in cells overexpressing Beclin 1-BD compared with Beclin 1-WT (Figures 4B and C). However, we did not detect differences among cells transfected with Beclin 1 mutant and cells overexpressing GFP or GFP-Rab11 as controls.

We next quantified the effect of the expression of Beclin 1-BD in *Cb* infection at earlier times after infection compared with vector-transfected cells. We observed that, as shown before, whereas in Beclin 1-WT-overexpressing cells the percentage of infection significantly increased compared with GFP-overexpressing cells (mainly at 6 h p.i.), overexpression of the Beclin 1 mutant markedly decreased the percentage of infected cells at both 6 and 12 h p.i. (Figures 4D). These results indicate that at early p.i. times, the CRV development is affected by the expression of this mutated form of Beclin 1, which is unable to interact with Bcl-2. In addition, the beneficial effect of Beclin 1 in *Cb* infection is apparently affected by the lack of communication between Beclin 1 and Bcl-2.

Bcl-2 colocalizes with the CRVs but alters the normal development of these vacuoles, without affecting the recruitment of Beclin 1 and LC3. Beclin 1 interacts with Bcl-2 through a BH3 domain that is present in Beclin 1.^{19,20} This interaction is reduced when autophagy is stimulated by nutrient deprivation, suggesting that the dissociation of the Beclin 1–Bcl-2 complex is important for autophagy

activation.²¹ In this study, we have shown that an adequate expression of Beclin 1 is required for the establishment of the large CRV; therefore, we analyzed whether Bcl-2 also has a

role in *Cb* infection. Figure 5A shows a cell overexpressing GFP-Bcl-2, which decorates the membrane of several CRVs. Panel d shows the graph of the fluorescence intensity



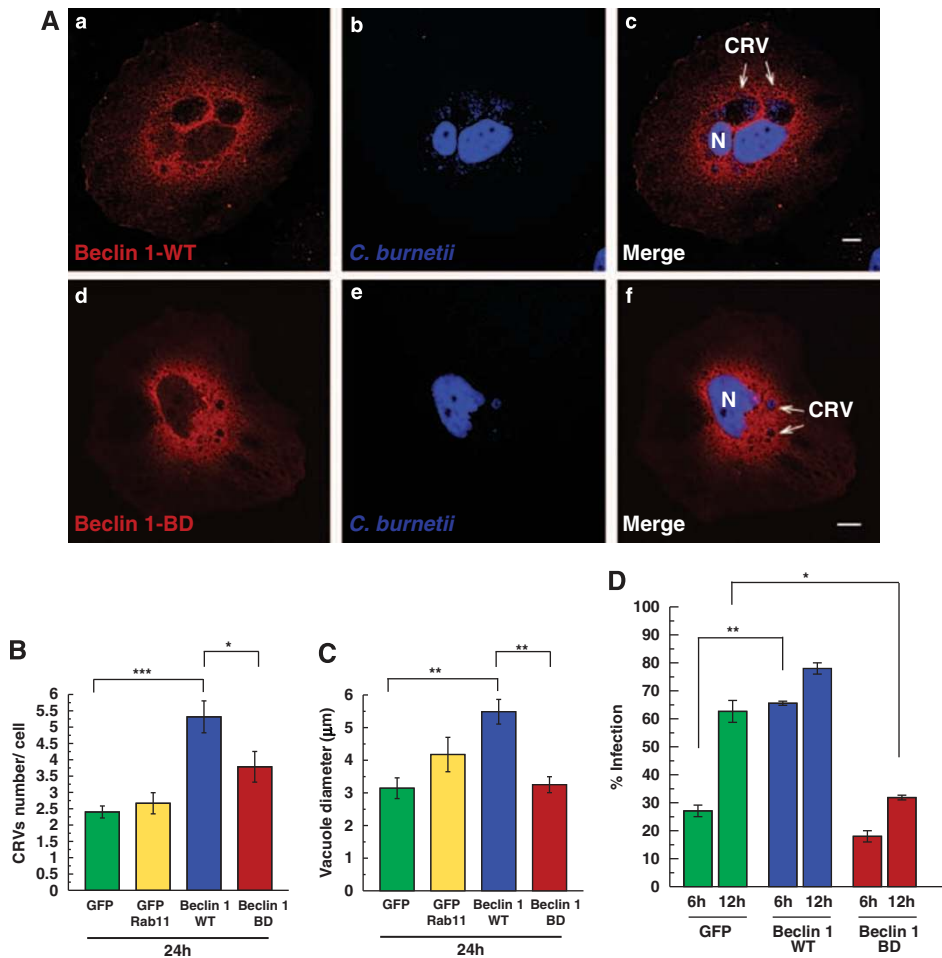
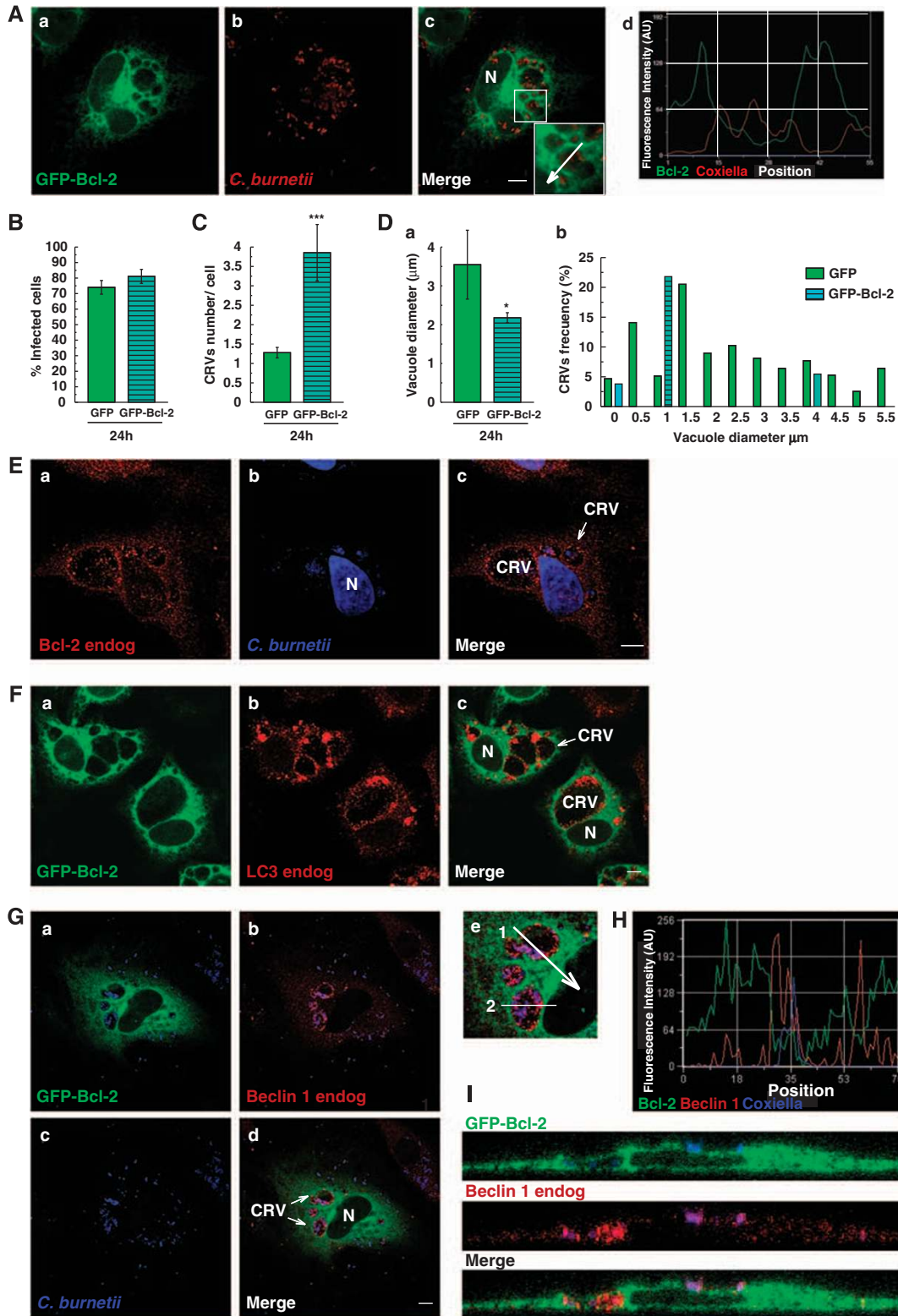


Figure 4 The beneficial effect of Beclin 1 in CRV development is not exerted by the mutant Beclin 1-BD. (A) Cells overexpressing Beclin 1-WT or Beclin 1-BD were infected with *Cb* for 24 h. Afterwards, cells were fixed and subjected to indirect immunofluorescence using specific antibodies. Panels a–c show cells overexpressing Beclin 1-WT detected with anti-FLAG and a secondary antibody conjugated to Texas red (panels a and c). *Cb* was detected with Hoechst staining (a DNA marker, blue in panels b and e). Panel c clearly shows Beclin 1 decorating the CRVs (arrows). Panels d–f show an infected cell overexpressing Beclin 1-BD detected with anti-Beclin 1 (red in panels d and f). Beclin 1-BD is also found decorating the small CRVs (arrow in panel f). N, nucleus. Scale bars: 10 μm. (B) Quantification of the number of CRVs per cell in cells overexpressing GFP, GFP-Rab11 (both as controls), Beclin 1-WT or Beclin 1-BD after 24 h p.i. Data represent means ± S.E.M. from at least three independent experiments. The CRVs number in transfected cells with Beclin 1-BD was (*) significantly different from cells overexpressing Beclin 1-WT, **P* < 0.05. (C) Quantification of vacuole diameter (μm) in the same cells as that in (b). Data represent means ± S.E.M. from at least three independent experiments. (D) Quantification of the percentage of infection in cells transfected with GFP (control), Beclin 1-WT or Beclin 1-BD after 6 and 12 h p.i. Note that after 6 h of infection, a marked increase in the percentage of infected cells is observed when Beclin 1-WT was expressed. In addition, a significant reduction of this parameter was observed in Beclin 1-BD-overexpressing cells even after 12 h p.i. Data represent means ± S.E.M., (*) and (**) significantly different from cells overexpressing GFP, **P* < 0.05, ***P* < 0.01. At least 100 cells were counted in each experiment

Figure 3 Beclin 1 depletion affects CRV development. (A) Diagram of the experimental design used. HeLa cells were infected with *Cb* for 3 h and transfected with the indicated plasmids. After 48 h, the cells were fixed and imaged. (B) Panels a–c show cells overexpressing GFP and endogenous Beclin 1 detected by indirect immunofluorescence using a specific antibody and an Alexa 546 labeled secondary antibody (red). Panels d–f show HeLa cells co-transfected with GFP and Beclin 1-KD to induce Beclin 1 depletion. The knockdown effectiveness was determined by indirect immunofluorescence using a specific antibody against Beclin 1. The arrows show CRVs. Scale bars: 10 μm. (C) Quantification of the number of CRVs per cell. Data represent means ± S.E.M., (*) significantly different from cells overexpressing FLAG-Beclin 1, **P* < 0.05. (D) Quantification of the vacuole size. Data represent means ± S.E.M., (**) significantly different from cells overexpressing GFP, ***P* < 0.01. (E) Diagram of the double-hit protocol. HeLa cells were transfected with the indicated plasmid. After 48 h cells, were subjected to a second transfection with the same plasmids, and incubated for additional 48 h. Subsequently, cells were infected with *Cb* for 24 h. (F) Determination of Beclin 1-knockdown by immunoblotting with anti-Beclin 1 antibody. (G) The confocal images, showing HeLa cells transfected with GFP (panels a–c) or with GFP and Beclin 1-KD (panels d–f) using the double-hit protocol, are described in (E). After 24 h of infection, cells were subjected to indirect immunofluorescence for detecting the bacterium and endogenous Beclin 1 levels. The arrows show CRVs. Scale bars: 10 μm. (H) Quantification of the number of CRVs per cell. Data represent means ± S.E.M., (*) significantly different, **P* < 0.05. (I) Quantification of the vacuole size. Data represent means ± S.E.M., (***) significantly different from cells overexpressing GFP, ****P* < 0.001. (J) Determination of autophagy response. HeLa cells were transfected with GFP-LC3 or GFP-LC3 and Beclin 1-KD by the double-hit protocol. After 2 h of incubation in full nutrient media (control) or starvation media (Stv), cells were fixed and the GFP-LC3-positive dots were analyzed using confocal microscopy. Note the reduction of GFP-LC3 dots in cells in which Beclin 1 was depleted (grey bars). Data represent means ± S.E.M. of at least two independent experiments, (****) significantly different from cells overexpressing GFP-LC3 alone, *****P* < 0.001 (number of counted cells = 100)



quantification along the white arrow across the CRV depicted in the inset, confirming the accumulation of Bcl-2 at the surrounding membrane. No differences were observed in the percentage of infected cells overexpressing GFP-Bcl-2 at 24 h p.i. (Figure 5B). However, a significant increase in the number of CRVs was detected in cells overexpressing GFP-Bcl-2 (Figure 5C), whereas the vacuole size was markedly reduced (Figure 5D, panel a). A distribution histogram of the vacuole size shows an increase in the small vacuole population in cells overexpressing Bcl-2 (Figure 5D, panel b).

To exclude the possibility that only overexpressed Bcl-2 was recruited to the membrane vacuole, the endogenous protein was detected. As shown in Figure 5E, endogenous Bcl-2 was also found decorating the CRV limiting membrane. These results indicate that Bcl-2 is targeted to CRVs and that overexpression of this protein leads to the formation of numerous CRVs, but of smaller size than in control cells.

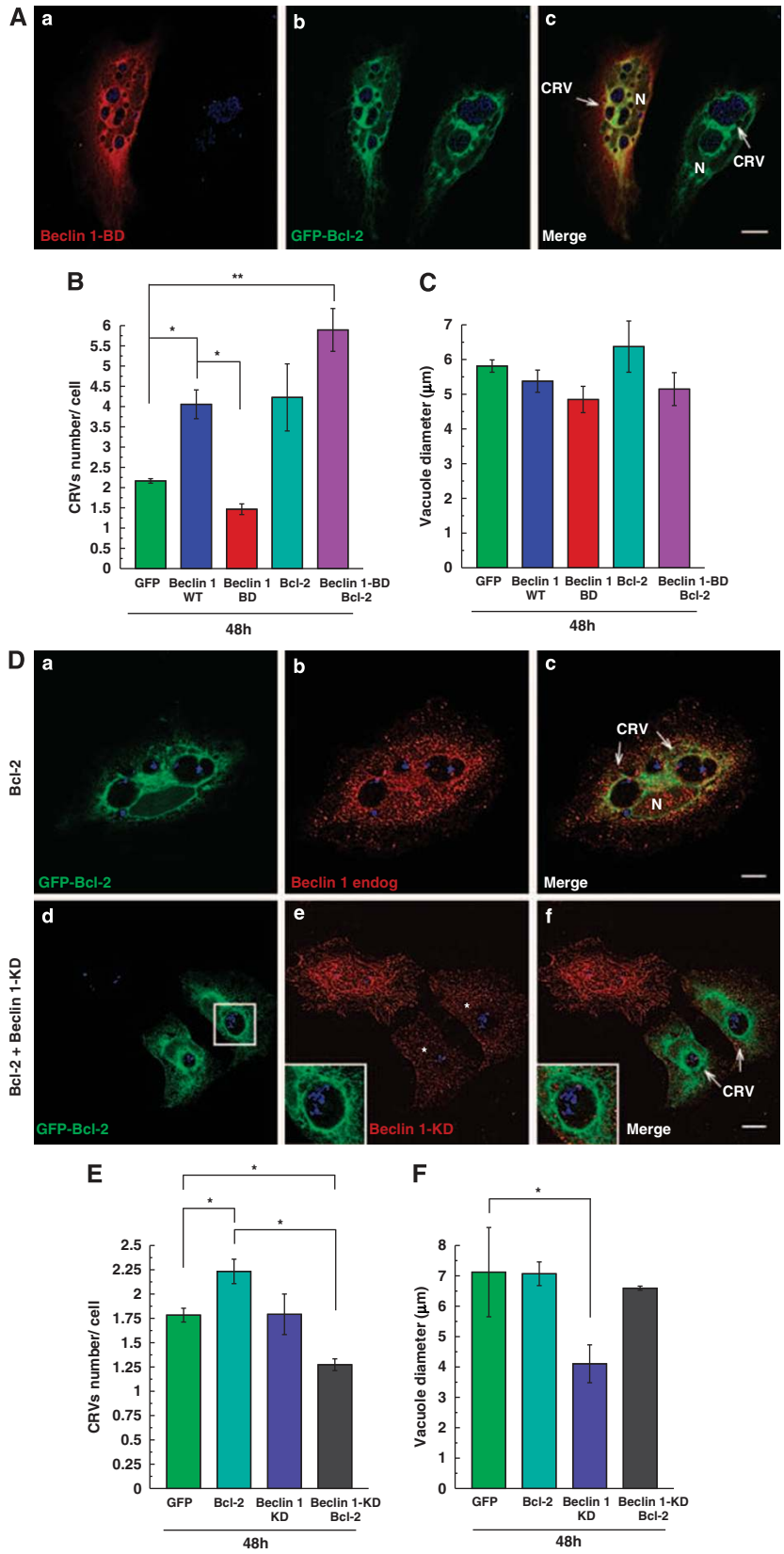
We next evaluated whether either LC3 or Beclin 1 was also associated with the CRVs in the cells overexpressing GFP-Bcl-2. Figure 5F shows that both GFP-Bcl-2 and endogenous LC3 were accumulated at the CRV membrane. In addition, the images depicted in Figure 5G, panels a–d, show the recruitment of GFP-Bcl-2 and endogenous Beclin 1 to the same CRV. Figure 5H shows the graph of the quantification of the fluorescence intensity along the white arrow across the CRV depicted in panel e, demonstrating the recruitment of both proteins at the surrounding membrane. Confocal microscopy analysis (Figure 5I) of midplane Z-sections through the center of the vacuole (see white line 2, in panel e) revealed that both proteins were indeed decorating the vacuole. The distribution pattern of endogenous Beclin 1 and LC3 suggests that despite the overexpression of Bcl-2 altered the normal establishment of the CRV, the autophagic proteins were still recruited.

As, *in vivo*, *Cb* has a tropism for the mononuclear phagocyte system, we also explored the distribution of either overexpressed Beclin 1-WT or GFP-Bcl-2 in a macrophage cell line (RAW cells) infected with *Cb*. Supplementary Figure 2, panel a, shows infected RAW cells with a marked recruitment of Beclin 1-WT (arrows in panel f) or GFP-Bcl-2 (arrows in

panel i) to the CRVs generated after 24 h p.i. In addition, the number of CRVs after 24 and 48 h of infection was highly increased in cells overexpressing either Beclin 1-WT or GFP-Bcl-2 compared with control GFP (Supplementary Figure 2, panels b and c). Therefore, our results indicated that both Beclin 1-WT and GFP-Bcl-2 have similar effects in macrophages to the ones observed in HeLa cells.

As indicated before, the CRVs are typically described as phagolysosomal structures characterized by the presence of lysosomal enzymes.²⁵ We have previously shown that early after infection, *Cb* phagosomes delay the arrival of the lysosomal enzymes. In addition, we have also presented evidence that the interaction with the autophagic pathway contributes to this delay, likely favoring bacterial replication.³⁰ It is believed that this delay benefits the transition from the SCV to the LCV form, which is the metabolically active and replicative competent bacterium. Therefore, to examine whether the compartment in which *Cb* survives was affected by the overexpression of the studied proteins in the present report, we analyzed the presence of the lysosomal enzyme, cathepsin D. For this purpose, cells were transfected with Beclin 1-WT, Beclin 1-BD, Bcl-2 or with the GFP vector as a control, and cathepsin D was detected by indirect immunofluorescence at 6 or 12 h p.i. (Supplementary Figure 3a). The images in panel S3A clearly show that the CRVs generated by *Cb* infection contain the lysosomal enzyme and the bacteria. When the percentage of CRVs containing cathepsin D was determined, we observed that by 6 h p.i. 80% of the vacuoles were labeled by the enzyme, whereas in the cells overexpressing Beclin 1-WT this percentage was decreased (panel S3b). Interestingly, these differences were lost at 12 h p.i. (panel S3c). No variations were observed in cells overexpressing either Beclin 1-BD or Bcl-2 at any p.i. time studied. The results suggest that overexpression of the fully functional Beclin 1 temporarily delays the fusion with lysosomes, likely to promote bacterial replication. Therefore, we next analyzed whether *Cb* survival was affected by the overexpression of Beclin 1-WT and its mutant form, or by overexpressed Bcl-2. As shown in panel S3d, the overexpressed Beclin 1-WT notably enhanced *Cb* replication and

Figure 5 Bcl-2 is recruited to the CRV, but alters its normal development. (A) HeLa cells overexpressing GFP-Bcl-2 were infected with *Cb* and at 24 h p.i., cells were fixed and subjected to indirect immunofluorescence using a rabbit anti-*Coxiella* (red) and a goat anti-rabbit Texas red. Cells were visualized using confocal microscopy (panels a–c). The images clearly show the generation of numerous Bcl-2 decorated vacuoles (panel c). Scale bars: 10 μ m. In panel c the inset is shown. Panel d shows the quantification of the fluorescence intensity along the white arrow in the inset of panel c. The white arrow in the merged image indicates the position and the direction of the profile line used for analysis. (B) Quantification of the percentage of infected cells in cells transfected with the vector alone (GFP) as a control and GFP-Bcl-2. (C) Quantification of CRVs number at 24 h p.i. Data represent means \pm S.E.M. from three independent experiments, (***) significantly different from cells overexpressing GFP, **** $P < 0.001$. At least 100 cells were counted in each experiment. (D) Panel a – Quantification of the vacuole diameter (μ m) at 24 h p.i. Data represent means \pm S.E.M. from at least three independent experiments, significantly different (*) from cells overexpressing GFP, * $P < 0.05$. At least 100 cells were counted in each experiment. Panel b – Vacuoles quantified in panel a, were groups according to their size and each group frequency is depicted in this panel. (E) Endogenous Bcl-2 also decorates the CRVs. Cells were infected with the bacterium for 48 h. After fixation, Bcl-2 was detected by indirect immunofluorescence using a specific antibody and a Texas rd labeled secondary antibody (panels a and c). *Cb* was detected using TOPRO, which labels both intracellular bacteria and host-cell nucleus (panel b). The arrows indicate the CRVs. N, nucleus. Scale bars: 10 μ m. (F) Endogenous LC3 localizes to the membranes of CRVs in transfected cells with GFP-Bcl-2. Cells were transfected with GFP-Bcl-2, then infected with *Cb* for 48 h and immunolabeled with a monoclonal antibody anti-LC3 (red). The images were analyzed using confocal microscopy. (G) HeLa cells overexpressing GFP-Bcl-2 were infected with *Cb*. At 48 h p.i., the cells were fixed and processed to detect endogenous Beclin 1 and the bacterium using specific primary antibodies goat anti-Beclin 1 and rabbit anti-*Coxiella*, respectively; anti-goat Alexa Fluor 546 and anti-rabbit Cy5 were used as secondary antibodies. Images were captured using a confocal microscope. Panel a shows CRV decorated with GFP-Bcl-2 and panel b depicts endogenous Beclin 1 (red) recruited to the vacuoles membrane. Panel d shows the merge image (arrows indicate the CRVs). Scale bars: 10 μ m. Panel e shows the inset with an arrow (1) to indicate the analysis of the fluorescence intensity, and a white line (2) indicating the plane analyzed as shown in Figure 4I. (H) The quantification of the fluorescence intensity along the white line 1 in panel e is shown. The arrow in the merged image indicates the position and direction of the profile line used for analysis. (I) These images shows a Z-stack of the white line 2 in the merged image acquired and subsequently processed. Images represent the transverse section of a CRV revealing both Beclin 1 and Bcl-2 recruited to the vacuole



viability as determined by an infectious focus-forming unit (FFU) assay. In contrast, overexpressed Bcl-2 or Beclin 1-BD failed to modify bacterial replication.

The biogenesis of the CRVs requires a proper relationship between Beclin 1 and Bcl-2. As our results indicate that overexpressed Bcl-2 increases the number of small CRVs and that Beclin 1-BD mutant alters the normal establishment of the CRVs, we analyzed whether the co-expression of Beclin 1-BD and GFP-Bcl-2 had an effect on CRV development. Figure 6A (panels a–c) shows an infected cell (left) co-transfected with Beclin 1-BD and GFP-Bcl-2 with an evident recruitment of both proteins to the vacuole membrane, and a cell (right) just transfected with GFP-Bcl-2. As previously shown in Figure 5C, overexpression of Bcl-2 highly increased the number of CRVs (Figure 6B, light blue bar) and this effect was not reverted by co-expression of the Beclin 1 mutant, unable to bind Bcl-2 (Figure 6B, violet bar). In contrast, the size of the vacuoles was not affected by overexpression of the different plasmids after 48 h of infection, indicating that the Bcl-2 effect on vacuole size is transient (Figure 6C).

In order to analyze these observations further, we used the plasmid Beclin 1-KD, which causes the knockdown of Beclin 1. We used the same experimental approach indicated in Figure 3A; the infected cells were transfected with the indicated plasmids and incubated for additional 48 h to suppress Beclin 1 expression. Figure 6D (panels d–f) shows cells co-transfected with GFP-Bcl-2 and Beclin 1-KD. In cells marked with asterisks (panel e), in which Beclin 1 depletion is clearly observed, overexpressed GFP-Bcl-2 colocalized with the CRV membrane (inset panels e and f), such as in cells in which endogenous Beclin 1 was not depleted (panels a–c). The number of CRVs per cell was reduced in cells co-expressing Bcl-2 and Beclin 1-KD compared with cells overexpressing either Bcl-2 or GFP (Figure 6E). However, overexpression of Bcl-2 reverted the vacuole diameter alteration caused by Beclin 1 depletion (Figure 6F, compare blue and black bars). Taken together, these results indicate that the recruitment of Bcl-2 to the vacuole membrane is

independent on the Beclin 1 presence. In addition, a proper ratio between Bcl-2 and Beclin 1 is required for the normal development of the CRVs.

The interplay between Beclin 1 and Bcl-2 is required for the anti-apoptotic effect of *Cb*. Cumulative evidence indicates that the apoptotic and autophagic pathways are interconnected.³⁶ Besides, the interaction of Beclin 1 and Bcl-2 has been implicated in the regulation of this crosstalk.³⁷ Recent results have shown that *Cb* infection is able to inhibit the apoptosis induced by UV light and staurosporine in host cells.^{34,35} As *Cb* infection is affected by Beclin 1 and Bcl-2, we wondered whether overexpression of these proteins would have an effect on the inhibition of apoptosis by *Cb*. Supplementary Figure 4a shows the basal percentage of the apoptotic nuclei of infected cells, transfected with the different plasmids treated or not with chloramphenicol (Ch), but unexposed to UV. Supplementary Figure 4b shows the anti-apoptotic effect of *Cb*, indicated by the significant difference observed between uninfected and infected cells overexpressing GFP and UV irradiated. Consistent with published observations,^{34,35} the apoptotic nuclei significantly increased in infected cells treated with Ch, showing that the anti-apoptotic function of *Cb* requires bacterial protein synthesis. The percentage of apoptotic nuclei in cells overexpressing GFP-Bcl-2 (Figure 7a, light blue bars), infected with *Cb* untreated or treated with Ch (bars 5 and 6) was similar to the infected cells overexpressing GFP (green bar 2), indicating that, as expected, overexpressed Bcl-2 has a protective role in the survival of the host cell. Interestingly, the anti-apoptotic effect of Bcl-2 was not affected by bacterial infection (compare light blue bars 4 and 5), suggesting that the *Cb* pro-survival activity is likely through Bcl-2. In contrast, no major differences were observed in cells overexpressing Beclin 1-WT (blue bars 7–9 compared with green bars 1–3), whereas in cells overexpressing Beclin 1-BD a marked increase of apoptosis in infected cells, untreated with Ch (red bar 11), was observed (compare bars 2, 8 and 11). This latter result indicates that in cells overexpressing the Beclin 1 mutant, the protective effect of *Cb* is lost. To confirm that the

Figure 6 The interplay between Beclin 1 and Bcl-2 is required for the biogenesis of the compartment in which *Cb* resides. **(A)** HeLa cells were doubly transfected with Beclin 1-BD and GFP-Bcl-2 and then infected with *Cb* for 48 h to allow vacuole formation. Afterward, cells were fixed and Beclin 1-BD and the bacterium were detected by indirect immunofluorescence using specific antibodies, anti-Beclin 1 (red) and anti-*Coxiella* (blue). Panels a–c show a cell overexpressing both proteins, in which mutant Beclin 1 and Bcl-2 (left) are found decorating the membrane of CRVs, and a cell overexpressing Bcl-2 alone (right). N, nucleus. Scale bar: 10 μ m. **(B)** Quantification of the number of CRVs per cell in cells doubly transfected with Beclin 1-BD and GFP-Bcl-2, and transfected with FLAG-Beclin 1, Beclin 1-BD, GFP-Bcl-2 or GFP as a control. Cells were infected for 48 h. Data represent means \pm S.E.M. from three independent experiments. At least 100 cells were counted in each experiment. The number of CRVs in cells co-expressing Beclin 1-BD and GFP-Bcl-2 were significantly different from the control GFP, $**P < 0.01$. The vacuole number in cells overexpressing FLAG-Beclin 1 was significantly different from Beclin 1-BD, $*P < 0.05$. **(C)** Quantification of vacuole diameter (μ m) in transfected cells with the indicated plasmids above and infected during 48 h. Data represent means \pm S.E.M. from at least three independent experiments. At least 100 cells were counted in each experiment. **(D)** HeLa cells were infected with *Cb* for 3 h and transfected with the indicated plasmids in the left. Next, cells were incubated for additional 48 h to allow Beclin 1 depletion. Panels a–c show cells overexpressing GFP-Bcl-2 infected with *Cb*. Endogenous Beclin 1 and the bacterium were detected by indirect immunofluorescence using anti-Beclin 1 (red) and anti-*Coxiella* (green). The white arrows indicate the recruitment of GFP-Bcl-2 and endogenous Beclin 1 to the membrane of the CRVs (panel c). Panels d–f show the infected cells doubly transfected with GFP-Bcl-2 and Beclin 1-KD to induce the suppression of Beclin 1. Then, cells were subjected to indirect immunofluorescence using specific antibodies against Beclin 1 (red), to determine the knockdown effectiveness, and against *Cb* (blue). The asterisks in panel e show two cells overexpressing GFP-Bcl-2 in which Beclin 1 has been knockeddown. Inset shows GFP-Bcl-2 decorating the membrane of a vacuole. The white arrows show CRVs. N, nucleus. Scale bars: 10 μ m. **(E)** Determination of the CRVs number in cells co-transfected with GFP-Bcl-2 and Beclin 1-KD (grey bar) and transfected with GFP-Bcl-2, Beclin 1-KD or GFP as a control. Data represent the mean \pm S.E.M. of at least three independent experiments (number of counted cells = 100). The percentage of CRVs in cells with Beclin 1 knockdown and overexpressed GFP-Bcl-2 was significantly different from control, $*P < 0.05$; and significantly different from cells overexpressing GFP-Bcl-2, $*P < 0.05$. **(F)** The vacuole size was quantified in the same cells. As expected, there was a significant difference only in cells with depleted Beclin 1 compared with control GFP, $*P < 0.05$; however, this reduction was reverted by Bcl-2 expression. Data represent the mean \pm S.E.M. of at least three independent experiments (number of counted cells = 100)

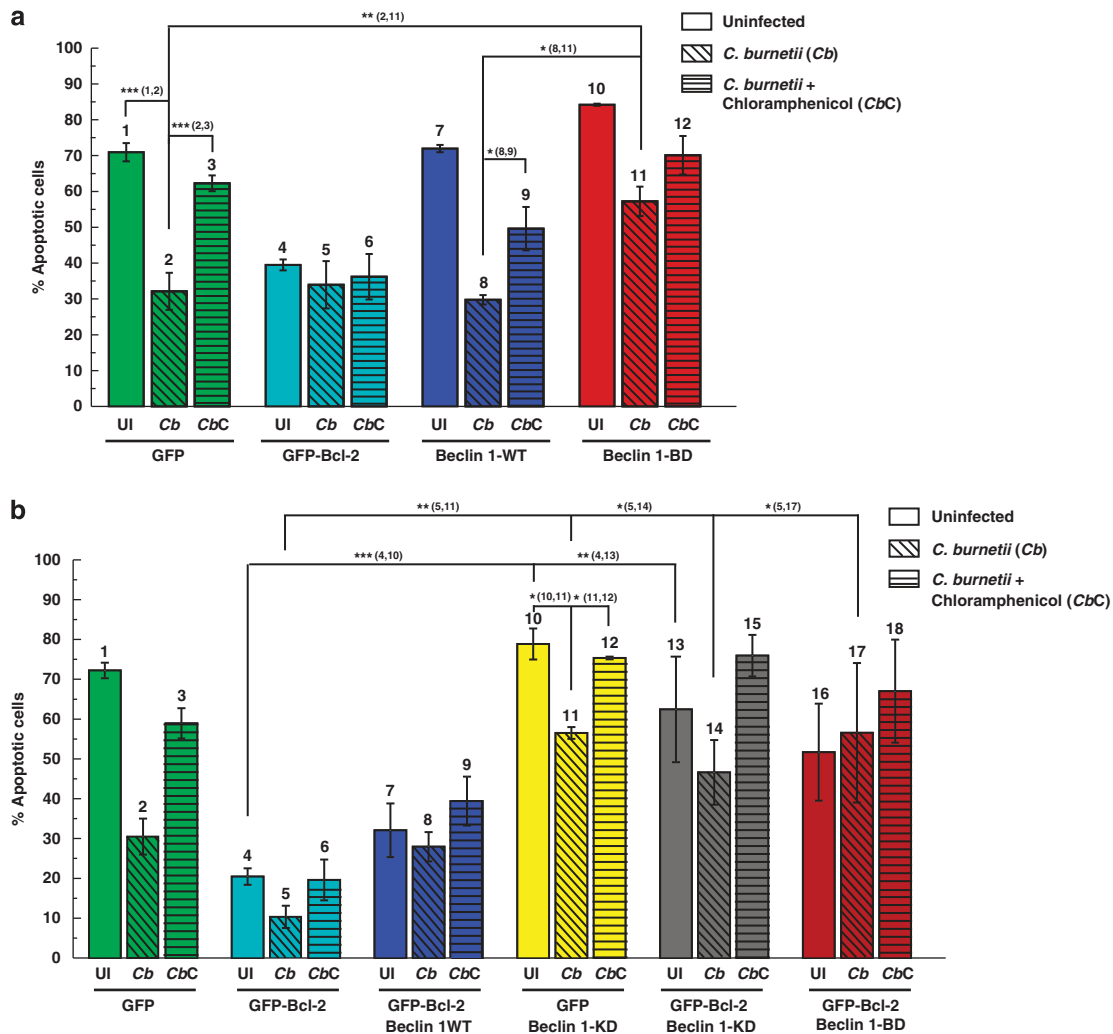


Figure 7 Interplay between Beclin 1 and Bcl-2 is required for the anti-apoptotic effect of *Cb*. (a) HeLa cells were transiently transfected with GFP (control), GFP-Bcl-2, FLAG-Beclin 1 (WT) or Beclin 1-BD. Afterward, the cells were left uninfected (UI) or infected with *Cb* for 24 h and treated with (CbC) or without (Cb) chloramphenicol (80 μ g/ml) for 18 h. Then, the cells were exposed to UV light for 15 min and incubated for 6 h at 37 °C. Cells were fixed and permeabilized to detect Beclin 1 and *Cb* with specific antibodies. The apoptotic nuclei were labeled with Hoechst and the percentage of apoptotic cells was determined. Data represent the mean \pm S.E.M. of three independent experiments in which at least 200 nuclei were scored in each experiment. The asterisks denote significant differences: * P < 0.05; ** P < 0.01; *** P < 0.001. (b) The knockdown of Beclin 1 blocks the anti-apoptotic activity of *Cb* and induces apoptosis. HeLa cells were left uninfected (UI) or infected with *Cb* for 3 h. Then, cells were transiently transfected with GFP (control, green bars) or GFP-Bcl-2 (light blue bars), or co-transfected with GFP-Bcl-2 and Beclin 1-WT (blue bars), GFP and Beclin 1-KD (to suppress the expression of endogenous protein) (yellow bars), GFP-Bcl-2 and Beclin 1-KD (grey bars) or with GFP-Bcl-2 and Beclin 1-BD (red bars). Cells were incubated for additional 24 h. Afterwards, the cells were treated with or without chloramphenicol (80 μ g/ml) for 18 h. Then, the cells were exposed to UV light for 15 min and incubated for 6 h at 37 °C. They were fixed and immunostained using specific antibodies against Beclin 1, to determine the knockdown effectiveness, and against *Cb*. The apoptotic nuclei were labeled with Hoechst and the percentage of apoptotic cells was quantified. Data represent the mean \pm S.E.M. of at least three independent experiments in which 200 nuclei were scored in each experiment. The asterisks denote significant differences: * P < 0.05; ** P < 0.01; *** P < 0.001

type of death was indeed apoptotic, we incubated the cells with Z-VAD-fmk (apoptosis inhibitor) for 2 h before UV irradiation. Supplementary Figure 4c shows that Z-VAD-fmk reduced apoptotic cell mortality in all cases. In addition, we corroborated these results using a TUNEL assay to detect apoptotic nuclei in cells overexpressing RFP (as control), Beclin 1-WT or Beclin 1-BD (Supplementary Figure 5). With this detection method the results obtained were very similar to the ones observed when the apoptotic nuclei were determined using Hoechst staining (compare Supplementary Figure 5b with Figure 7a).

We next assessed whether *Cb* was able to prevent cell death when Beclin 1 expression was reduced (Figure 7b). Infected and uninfected cells were transfected with GFP (green bars 1–3), GFP-Bcl-2 (light blue bars 4–6) or co-transfected with GFP-Bcl-2 and Beclin 1-WT (blue bars 7–9) or BD mutant (red bars 16–18). To suppress Beclin 1, cells were also co-transfected with Beclin 1-KD and GFP (yellow bars 10–12), or with Beclin 1-KD and GFP-Bcl-2 (grey bars 13–15), and then exposed to UV light. When Beclin 1-WT and GFP-Bcl-2 were co-expressed, the number of apoptotic cells was similar to the cells overexpressing GFP-Bcl-2 alone

(compare light blue and blue bars). Interestingly, the apoptotic nuclei highly increased in infected cells depleted of Beclin 1 overexpressing either GFP or GFP-Bcl-2, compared with cells overexpressing only GFP-Bcl-2 (Figure 7b, compare hatch bar 5 with 11 and 14). In addition, the mutant protein of Beclin 1, which was unable to interact with Bcl-2, not only prevented the anti-apoptotic effect of Bcl-2, but also the one induced by *Cb* infection (compare bars 4 with 16 and 5 with 17, respectively). Similarly, the anti-apoptotic effect of overexpressed Bcl-2 was lost in Beclin 1-depleted cells (compare uninfected bars 4 and 13). These results support the idea that a proper relationship between Beclin 1 and Bcl-2 is necessary for the inhibition of apoptosis by *Cb*. Furthermore, these findings suggest that the anti-apoptotic effect of Bcl-2 requires the presence of a fully functional Beclin 1.

Discussion

To date, very little is known about the role of Beclin 1 in pathogen infections. In this study, we present evidence that *Cb* infection induces the recruitment of endogenous and overexpressed Beclin 1 to the large CRV, even at extended p.i. times (Figure 1). These observations are consistent with our previous results that two other proteins involved in autophagy, LC3 and Rab24, decorate the CRV.²⁹ In addition, we observed that both Beclin 1 and LC3 were clearly decorating the same vacuole membrane. Interestingly, our data show that the development of CRVs was favored by Beclin 1 expression, indicated by the increase in the number and size of CRVs in cells overexpressing Beclin 1 (Figure 1). These findings support the concept that *Cb* exploits autophagy to its own benefit and that overexpression of proteins involved in this process are enriched at the CRV membrane. It is noteworthy the presence of Beclin 1 in a compartment with the phagolysosomal characteristics of CRVs, given that Beclin 1 is required at early events, as the nucleation of pre-autophagosomal structures.⁵ We have observed colocalization of endogenous Beclin 1 with Rab7 at the membrane of the CRVs at 48 h after infection, consistent with the late/lysosomal nature of this compartment (data not shown).

Interestingly, using the probe GFP-2xFYVE that binds to PI3P, the PI3-kinase product, our results indicate that the Beclin 1/hVps34 complex recruited to the CRV membrane was functionally active at all times analyzed (Figure 2). These data suggest an active engagement of the autophagic and endocytic/phagocytic pathways during *Cb* infection, in order to thrive on the harsh environment in which this bacterium survives. A recent publication³⁸ shows that Toll-like-receptor (TLR) signaling induces the association of autophagic proteins to the phagosome, apparently without autophagosome formation, enhancing the fusion with lysosomes and, subsequently, leading to the degradation of the engulfed organism. As *Cb* actually replicates in a lysosomal-like compartment, our earlier^{29,30} and present data suggest that the recruited autophagic proteins are effectively and efficiently used to promote *Cb* survival. Indeed, we have observed that in cells overexpressing Beclin 1, there was a delay in the arrival of the lysosomal enzyme, cathepsin D (Supplementary Figure 3b), which likely favors bacterial growth. In addition, the results presented in this report indicate that at early p.i. times,

overexpression of Beclin 1 enhances the percentage of *Cb*-infected cells (Supplementary Figure 1a) and promotes bacterial replication (Supplementary Figure 3d).

In addition, we have observed that the knockdown of Beclin 1 leads to a reduction in the number and size of the generated CRVs (Figure 3). These results indicate that Beclin 1 is required for the normal establishment of CRVs, confirming the positive effect of autophagy in *Cb* infection, as a reduced number of LC3-positive dots was observed in Beclin 1-suppressed cells (Figure 3J), corroborating that reduced levels of Beclin 1 by siRNA lead to an inhibition of autophagy.¹⁸

As indicated above, Beclin 1 promotes autophagy by acting as a platform for the formation of the complex with hVps34 and several interacting proteins that positively regulate autophagy. Moreover, Beclin 1 possess a BH3 domain that allows the interaction with the anti-apoptotic proteins, Bcl-2 and Bcl-X_L.^{19,20} In this report, we have observed that both endogenous and overexpressed Bcl-2 were clearly decorating the membrane of the CRV (Figures 5A–E). In addition, the overexpressed Bcl-2 increased the number of CRVs but the vacuole size was reduced (Figures 5C and D). However, at 48 h of infection the vacuole size was comparable with the control GFP (Figure 6C), suggesting that excess Bcl-2 somehow alters CRV development early at infection. This would be consistent with the observation that overexpressed Bcl-2 interferes with the formation of the Beclin 1/hVps34 complex.²¹ Indeed, the colocalization of Bcl-2 with the CRV membrane was unexpected, considering that no previous reports have indicated the recruitment of Bcl-2 to a pathogen-containing compartment. It is intriguing that the CRV was decorated not only by GFP-Bcl-2, but also by endogenous Beclin 1 and LC3 (Figures 5F–I), strongly suggesting an active engagement with autophagy. These results may seem paradoxical because, as indicated above, Bcl-2 is capable of inhibiting starvation-induced autophagy.²¹

We have analyzed the development of CRVs in cells transfected with a mutant of Beclin 1 (Beclin 1-BD), which is defective in Bcl-2 binding. Our data showed that Beclin 1-BD was indeed recruited to the membrane of the CRV, but it decreased the percentage of infection (Figures 4A and D, respectively). Pattingre *et al.*²¹ showed that Beclin 1-BD induces excessive levels of autophagy in nutrient-rich conditions, leading to autophagic cell death, suggesting that the Bcl-2 interaction with Beclin 1 is crucial to avoid inappropriate autophagy activation. Indeed, Gottlieb and collaborators³⁹ showed that under rich- and low-nutrient conditions, the Beclin 1-BD expression impairs the normal autophagic flux, preventing the autolysosomal clearance rather than increasing autophagy. This suggests that Beclin 1-Bcl-2 interaction is required to promote autophagy. Given that autophagy benefits *Cb* infection and bacterial replication, the altered infection pattern observed in Beclin 1-BD-expressing cells can be explained by a defective autophagic pathway. Interestingly, in infected cells co-transfected with GFP-Bcl-2 and Beclin 1-KD (to deplete the endogenous protein), we have observed that GFP-Bcl-2 was present on the CRV membrane even in cells in which Beclin 1 was suppressed. However, the number of CRVs in these cells decreased (Figures 6D–F). Therefore, despite that either Beclin 1 or

Bcl-2 are independently recruited to the vacuole membrane, we propose that both proteins are necessary for the proper establishment of the CRV, likely by the regulation of adequate autophagy levels and normal flux.

Several pathogens have developed different strategies to govern the fate of the host cells. For example, *Chlamydia trachomatis* and *Toxoplasma gondii* are known to possess anti-apoptotic activity.^{40,41} Recently, it has been shown that a substrate (SidF) of the Dot/Icm T4SS is involved in preventing apoptosis in infected cells with *Legionella pneumophila*. Apparently, SidF would abolish the activities of two pro-apoptotic proteins members of the Bcl-2 family: BNIP3 and Bcl-rambo.⁴² Similarly, recent studies show that *Cb* inhibits apoptosis induction in host cells and this effect is mediated by the bacterial protein synthesis.^{34,35} Cumulative evidence indicates that apoptosis and autophagy are interconnected pathways, implying that a common stimulus triggers the response of both pathways or that the activation of one of them excludes the other.³⁶ Consequently, we explored a possible role for Beclin 1 and Bcl-2 in the anti-apoptotic effect of *Cb*. Our results revealed that *Cb* infection protects host cells overexpressing GFP, as well as Beclin 1-WT, of apoptotic cell death and this effect was dependent on an active bacterial protein synthesis (Figure 7a). It is noteworthy that in infected cells overexpressing GFP-Bcl-2, the number of apoptotic nuclei was similar to the control (GFP cells); however, treatment of the cells with Ch did not yield differences compared with untreated cells (Figure 7a), indicating that overexpressed Bcl-2 compensates the anti-apoptotic activity of *Cb* having a protective role in the survival of the host cell. On the other hand, a marked increase in apoptotic nuclei was observed in infected cells overexpressing Beclin 1-BD, indicating that the anti-apoptotic effect of *Cb* is abolished by the presence of the Beclin 1-BD mutant (Figure 7a). Altogether, these results suggest that the anti-apoptotic activity of *Cb* requires an appropriate interplay between Beclin 1 and Bcl-2. Therefore, it is tempting to speculate that a protein(s) synthesized by *Cb* or effectors of the *Cb*-T4SS are necessary to maintain the link between Beclin 1 and Bcl-2, to induce autophagy and prevent apoptosis, preserving both the integrity and the metabolic activities of the infected cell and allowing the normal development of the CRV. Thus, the results of this study in the *Cb*-infected cells seem somehow contradictory to previous results showing that overexpressed Bcl-2 inhibits starvation-induced autophagy.²¹ However, another report has indicated that overexpressed Bcl-2 or Bcl-X_L increases autophagy in MEF cells *Bax/Bak*^{-/-} treated with etoposide.⁴³ Consequently, it is probable that the regulatory effect of the Beclin 1-Bcl-2 complex depends on the nature of the stimulus; in our case, it is tempting to speculate that *Cb* would be modulating the activity and the relationship between both proteins for its own benefit and survival.

To support our model, we suppressed the endogenous Beclin 1 (Beclin 1-KD) and overexpressed GFP or GFP-Bcl-2 in the same infected cells to subsequently evaluate apoptosis. As expected, a marked increase in apoptotic cell death was observed in infected cells with Beclin 1 depleted (Figure 7b, yellow bars). However, the anti-apoptotic effect of *Cb* was also lost in cells doubly transfected with GFP-Bcl-2 and Beclin 1-

KD (Figure 7b, grey bars). In addition, cells co-transfected with GFP-Bcl-2 and Beclin 1-BD also presented a marked increase in the apoptotic nuclei (red bars). Thus, these results confirm our hypothesis that the intracellular survival of *Cb* and the persistence of this bacterium in the host cell require a proper interplay between Beclin 1 and Bcl-2. Interestingly, when cell death was determined in uninfected cells, overexpression of Bcl-2 was unable to protect cells from apoptosis in Beclin 1-suppressed cells or in cells co-expressing the Beclin 1 mutant unable to interact with Bcl-2 (compare bars 4, 13 and 16 in Figure 7b), suggesting that Beclin 1 would be modulating the anti-apoptotic action of Bcl-2. This notion is supported by results obtained in myeloid leukemia cells, in which the knockdown of Beclin 1 activates apoptosis.⁴⁴ These researchers have shown that Beclin 1 acts as a negative regulator of apoptosis because it competes with the pro-apoptotic protein Bad, for binding to the anti-apoptotic protein Bcl-X_L, implying that the complex Beclin 1-Bcl-X_L has indeed an anti-apoptotic role.⁴⁴ In addition, it has recently been reported that dexamethasone induces autophagy in murine T-cell lymphoma line. Furthermore, this autophagy induction is enhanced by Bcl-2 overexpression, apparently because of the inhibition of dexamethasone-induced apoptosis.⁴⁵ Also, a recent publication shows that overexpressed Beclin 1 does not prevent the anti-apoptotic effect of Bcl-2.⁴⁶ This is consistent with the results that we have obtained in cells co-expressing Bcl-2 and Beclin 1-WT (see Figure 7b, blue bars). Thus, it is likely that the interplay between apoptosis and autophagy would be dependent on the different stimulus, in order to lead to survival or cell death, according to the desired beneficial effect.

According to the data discussed above, we propose a working model to explain the behavior of *Cb* during infection (Figure 8). *Cb* is internalized by phagocytosis but induces autophagy in the host cell. At very early p.i. times, the phagosome fuses with autophagosomes, recruiting LC3 and the Beclin 1/hVps34 complex. This interaction with the autophagic pathway delays the arrival of the lysosomal enzymes, allowing the residence of *Cb* in a less harmful compartment and the transition from SCV to LCV.^{29,30} Then, the phagosomes fuse with late endosome/lysosomes, generating the large CRV that occupies almost the whole cell, in which *Cb* survives. However, the establishment of this infection does not hamper host cell viability. Thus, *Cb* is able to produce a persistent infection by means of inhibiting apoptosis.^{34,35} Interestingly, we have observed that in *Cb*-infected cells numerous mitochondria are in close apposition to the CRV (Colombo MI *et al.* unpublished observation). This intimate association suggests that the bacteria may actively manipulate critical mitochondria functions, such as the intrinsic apoptotic pathway. Therefore, we propose that the anti-apoptotic effect of *Cb* is due, at least in part, to the recruitment of Bcl-2 to the vacuole membrane and to the modulation of Bcl-2 by Beclin 1. Once the *Cb* infection has been settled, a fraction of Beclin 1 and Bcl-2 would be interacting at the vacuole membrane and probably at the outer mitochondria membrane, preventing the binding of sensitizer pro-apoptotic proteins (e.g. BH3-only proteins) to Bcl-2 and thus inhibiting the activation of Bax/Bak and the release of cytochrome c. Recent evidence has shown that *Cb* leads to a

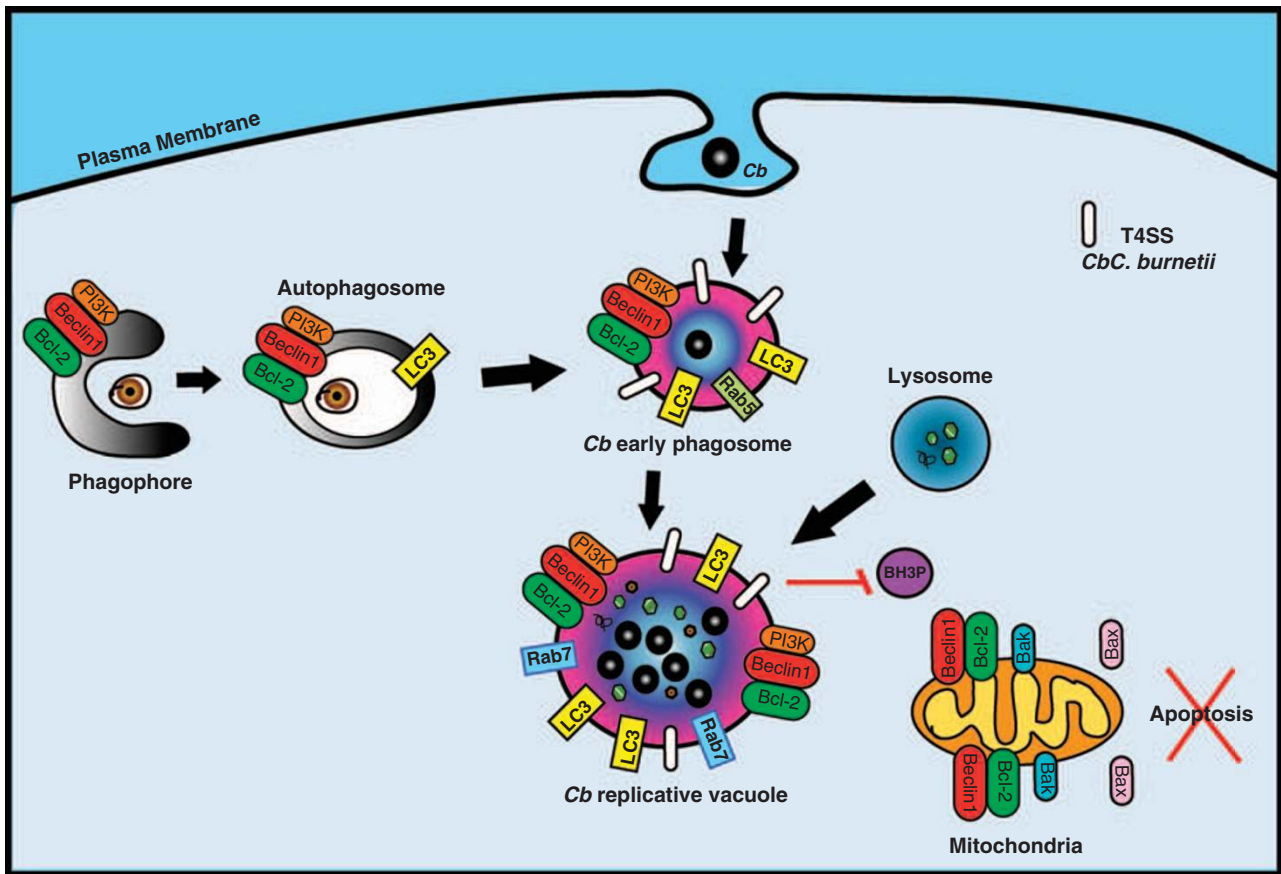


Figure 8 Modulation of the autophagy and apoptosis pathways by *Cb*. *Cb* is internalized into the host cell after a classical phagocytosis. Autophagy pathway is induced, probably through injected proteins through the T4SS of *Cb*. Thus, the compartment containing *Cb* fuses with autophagosomes, acquiring autophagic key proteins, such as LC3, Rab24 and Beclin 1, which favor the generation of the large replicative vacuoles in which *Cb* survives and multiplies. Moreover, *Cb* also establishes a persistent infection by means of inhibiting apoptosis in infected cells. This anti-apoptotic effect of *Cb* is due, at least in part, to the recruitment of the anti-apoptotic protein Bcl-2 to the membrane vacuole. In concert with Beclin 1, the binding of pro-apoptotic proteins (e.g. BH3-only proteins) to Bcl-2 is avoided and, therefore, the triggering of apoptosis is inhibited

sustained activation of Akt and Erk1/2 pathways.⁴⁷ It is known that Akt is a pro-survival kinase that inhibits activation of pro-apoptotic mitochondrial proteins and transcription factors.⁴⁸ Consistent with this finding, it is likely that the protein(s) secreted by the *Cb*-T4SS might be inhibiting a BH3-only protein activity and therefore the binding of this protein to Bcl-2. Thus, Beclin 1 is a crucial regulator of autophagy and apoptosis in infected cells, because of its role as a member of the Beclin 1/Vps34 complex and its participation in the anti-apoptotic complex Beclin 1-Bcl-2, competing with Bad for the binding to Bcl-2.⁴⁴

To summarize, the data presented here show that *Cb* infection is favored by overexpressed Beclin 1 and that depletion of this protein, as well as of the overexpressed Bcl-2, alters the normal development of CRVs. Furthermore, our results suggest the existence of a functional interaction between the autophagic and apoptotic pathways in infected cells, to avoid apoptosis induction and to trigger the autophagy pathway, allowing the survival and development of *Cb*. In addition, the present report emphasizes the importance of exploiting the infection with a microorganism to study a complex process, which allowed us to show a key role of Beclin 1 and Bcl-2 in modulating the fate of the cells.

Materials and Methods

Materials. DMEM medium was obtained from Gibco (Invitrogen, Buenos Aires, Argentina) and fetal bovine serum (FBS) from Natocor (Córdoba, Argentina). Plasmids pSG5-FLAG- epitope-tagged human Beclin 1 and pCR3.1 Beclin 1-BD were kindly provided by Dr. Beth Levine (Columbia University, New York, USA). pEGFP-LC3 was generously provided by Dr. Noboru Mizushima (Department of Physiology and Cell Biology, Tokyo Medical and Dental University, Tokyo, Japan) and Dr. Tamotsu Yoshimori (Department of Cellular Regulation, Research Institute for Microbial Diseases, Osaka University, Suita, Osaka, Japan). pGFP-Bcl-2 was provided by Dr. Michel Rabinovitch (Escola Paulista de Medicina, Sao Paulo, Brazil) and pGFP-FYVE by Dr. Sergio Grinstein (Hospital of Sick's Kids, Toronto, Canada). pBeclin 1-KD (pSuper.retro.puro vector in which the oligonucleotide sequence used for siRNA interference with Beclin1 expression has been inserted) was provided by Dr. William S Maltese (Medical University of Ohio, Toledo, Ohio, USA). The antibodies used in this work were rabbit polyclonal anti-*Coxiella*, generously provided by Dr. Robert Heinzen (Rocky Mountain Laboratories, NIH, MT, USA), and monoclonal mouse anti-LC3 developed in our lab. Beclin 1 was detected with goat anti-Beclin 1 (Santa Cruz Biotechnology, Inc., CA, USA) and an antibody against FLAG (Sigma, Buenos Aires, Argentina). Endogenous Bcl-2 was detected with a rabbit anti-Bcl-2 (Chemicon International, CA, USA). Rabbit anti-cathepsin D was kindly provided by Dr. Maximiliano Gutierrez (Helmholtz Centre for Infection Research, Germany). Mouse anti-Actin was from BD (Franklin Lakes, NJ, USA). The secondary antibodies were donkey anti-rabbit conjugated to Cy5, donkey anti-goat conjugated to Cy3, donkey anti-rabbit conjugated to HRP, donkey anti-goat conjugated to HRP and donkey anti-mouse conjugated to HRP (Jackson ImmunoResearch Laboratories, PA, USA). Other secondary antibodies used

were goat anti-rabbit conjugated to Texas red and goat anti-mouse conjugated to Cy3 from Amersham Biosciences Argentina SA (Buenos Aires, Argentina). The secondary antibody goat anti-rabbit conjugated to Alexa Fluor 488 and the DNA markers, Hoechst 33258 and TOPRO, were obtained from Molecular Probes (Invitrogen). Z-VAD-fmk, the Earle's balanced salts solution, EBSS (starvation) media and vinblastine were from Sigma. TUNEL assay was from Promega (Madison, WI, USA).

Cell culture and propagation of *Cb* phase II. HeLa cells were maintained in DMEM 10% FBS (full nutrient medium) at 37 °C in an atmosphere of 95% air and 5% CO₂.

Clone 4 phase II Nine Mile strain of *Cb* bacteria, which are infective for cells but not for mammals, were provided by Ted Hackstadt (Rocky Mountain Laboratories). Non-confluent Vero cells were cultured in T75 flasks at 37 °C in DMEM medium supplemented with 10% FBS, 0.22 g/l sodium bicarbonate and 20 mM Hepes, pH 7 (infection media). Cultures were infected with phase II *Cb* suspensions for 7 days at 37 °C. Afterwards, cells were lysed, scrapped and centrifuged at 800 *g* for 10 min at 4 °C to eliminate cellular debris. The supernatants were centrifuged at 24 000 *g* for 30 min at 4 °C, and pellets containing *Cb* were resuspended in DMEM, passed 20 times through a 27-gauge needle connected to a syringe, aliquoted and frozen at -70 °C.

Cell transfection. HeLa cells were transfected with the indicated plasmid (1 mg/ml) using LipofectAMINE 2000 (Invitrogen) as indicated by the manufacturer. The transfected cells were incubated for 24 h in DMEM supplemented with 10% FBS in 24-well plates at 80% confluence and then infected.

Infection of HeLa cells with *Cb*. HeLa cells grown in a T25 flask were washed three times with PBS and detached with trypsin-EDTA. After resuspending with infection media, cells were plated on coverslips distributed in 24-well plates. Subsequently, cells were transfected with the corresponding plasmids. For long infection times, 120 μ l aliquot of *Cb* suspension was diluted with 12 ml of infection media, and 500 μ l of the dilution was added per well. With this dilution an MOI of 10 was obtained.²⁹ Cells were centrifuged at 500 *g* for 10 min and incubated for different periods of time at 37 °C in an atmosphere of 95% air and 5% CO₂. Cells were fixed and analyzed using indirect immunofluorescence as described below.

Infection with *Cb* and Beclin 1 knockdown with the plasmid pBeclin 1-KD. HeLa cells were plated in 24-well plates at 80% confluence and then infected with *Cb*. A 200 μ l aliquot of *Cb* suspension was diluted in 12 ml of infection media, and 0.5 ml of this dilution was added per well (an MOI of 50). Cells were centrifuged at 500 *g* for 10 min and incubated for 3 h at 37 °C. Afterwards, cells were washed three times with PBS to eliminate extracellular bacteria and transfected with pGFP (as a control) or co-transfected with pBeclin 1-KD and pGFP or with pBeclin 1-KD and pGFP-Bcl-2, in another set of experiments. Cells were incubated for 48 h at 37 °C to knockdown Beclin 1 expression and to allow the development of the CRVs. The cells were fixed and analyzed using indirect immunofluorescence as described below.

Double-hit protocol. HeLa cells were plated in six-well plates at 40% confluence and then transfected with GFP (control) or GFP and Beclin 1-KD. After 48 h, cells were transfected for a second time with the same plasmids. Cells were incubated for additional 48 h and infected with *Cb* during the last 24-h period. Next, cells were fixed and subjected to indirect immunofluorescence as described below. To check knockdown efficiency, transfected cells were processed to detect endogenous Beclin 1 using western blot assays (described below).

Autophagy assays. To check autophagy activity in Beclin 1-depleted cells, cells were transfected with either Beclin 1-KD and GFP-LC3 or GFP-LC3 by the double-hit protocol. Then, cells were subjected to starvation for 2 h to induce autophagy. Afterward, cells were fixed and analyzed using indirect immunofluorescence detecting endogenous Beclin 1 as described below. The number of GFP-LC3-positive dots per cell was determined in starved cells compared with the same cells but incubated with full nutrient media. The GFP-LC3-positive dots were scored using ImageJ software (NIH, Bethesda, MD, USA).

Indirect immunofluorescence. HeLa cells were fixed with 0.5 ml of 3% paraformaldehyde solution in PBS for 10 min at room temperature, washed with PBS and quenched with NH₄Cl 50 mM in PBS for 20 min. Then, cells were

permeabilized with 1% saponin in PBS containing 1% BSA (blocking buffer). After blocking, cells were incubated with the indicated primary antibodies for 1 h. The cells were washed three times in blocking buffer and subsequently incubated with the indicated fluorophore-conjugated secondary antibody for 1 h.

For double immunolabeling, primary antibodies against *Cb* phase II (1 : 800) and against FLAG (1 : 200) were used. Bound antibodies were detected by incubation with secondary antibodies: goat anti-rabbit conjugated with Alexa 488 (1 : 600) or goat anti-mouse Cy3 (1 : 800), respectively. Endogenous LC3 was detected with a monoclonal antibody developed in our lab (1 : 10). Endogenous Beclin 1 was detected with a goat anti-Beclin 1 (1 : 50). Endogenous Bcl-2 was detected with a rabbit anti-Bcl-2 (1 : 100). Endogenous cathepsin D was detected with a rabbit anti-cathepsin D (1 : 50). Coverslips were mounted on glass slides using Mowiol (Calbiochem-Merck, Darmstadt, Germany), Mowiol-Hoechst 33258 or Mowiol-TOPRO (Molecular Probes, Invitrogen) and examined using fluorescence confocal microscopy.

Fluorescence microscopy. HeLa cells transfected with the different plasmids were analyzed by confocal microscopy using a Nikon C1 Confocal Microscope System or a FV100 Olympus Confocal Microscope (Olympus, Tokyo, Japan). Images were processed using Adobe CS (Adobe Systems Inc., San Jose, CA, USA), ImageJ software, Metamorph Program, series 4.5 (Universal Images Corporation, Tokyo, Japan), EZ-C1 program (Nikon, Tokyo, Japan) and FV10-ASW program (Olympus, Japan). For apoptosis assays an inverted microscope (Nikon Eclipse 2000, Japan) and a FV100 Olympus Confocal Microscope (Olympus, Japan) were used. Images were obtained using a CCD camera (Orca I, Hamamatsu, Hamamatsu City, Japan) and processed using the Metamorph Program, series 4.5 (Universal Images Corporation).

Measurements of the percentage of infected cells, number and size of CRVs. At different times after infection, cells were fixed for 10 min in 3% paraformaldehyde. At least 100 cells were scored in, at least, three independent experiments. The percentage of infection was calculated as the ratio between the number of infected cells and the number of total cells counted. Infected cells were defined as those with at least one clear identifiable bacterium inside. The number and size of vacuoles was determined by a morphometric analysis using Adobe Photoshop CS program (Adobe Systems Inc.) and EZ-C1 program (Nikon, Japan).

Bacterial viability and replication. The effect of overexpressed Beclin 1-WT, Beclin 1-BD and GFP-Bcl-2 on *Cb* replication and viability were quantified using a fluorescent infectious FFU assay on Vero cell monolayers as described.⁴⁹ In brief, transfected HeLa cells were infected for 24 h and then lysed by several passages through a 27-gauge needle connected to a syringe, a step that does not reduce the bacterial infectivity. Lysates were sonicated and serially diluted, and used to infect monolayers of Vero cells grown on coverslips in 24-well tissue culture plates in infection media at 37 °C in a 5% CO₂ atmosphere. At 48 h after infection, Vero cells were washed with PBS, fixed in 3% paraformaldehyde and processed for immunofluorescence with a rabbit anti-*Coxiella* antibody as described above. The average number of FFU in 50 fields was determined for each sample using a FV100 Olympus Confocal Microscope (Olympus, Japan). Approximately 500 cells were scored per coverslip. The cells were scored using ImageJ software.

Western blot analysis. To detect the knockdown efficiency of Beclin 1-KD, HeLa cells were transfected after the double-hit protocol with GFP alone or with GFP and Beclin 1-KD. After 72 h of the second transfection, cells were washed, scraped, resuspended in sample buffer containing 1% 2-mercaptoethanol and sonicated for 10 min at 4 °C. The samples were frozen until use. For western blots analysis, the protein extracts were subjected to electrophoresis in 12.5% SDS-PAGE gels, transferred to a nitrocellulose membrane and blocked with PBS supplemented with 0.1% v/v of Tween-20 and 5% of milk. The nitrocellulose membrane was incubated for 2 h with a goat anti-Beclin 1 (1 : 200), washed and incubated with a secondary HRP-conjugated anti-goat antibody (Jackson ImmunoResearch Laboratories) at a 1 : 10 000 dilution. Equal proteins loading were confirmed using mouse anti-Actin antibody (1 : 10 000). The bands were visualized using the ECL reagent (GE Healthcare, Buckinghamshire, UK), and analyzed using ImageJ software.

To detect LC3 conversion in *Cb*-infected cells, HeLa cells were infected or left uninfected for 48 h. Uninfected cells were subjected to control conditions, starvation with EBSS media for 2 h or starvation and 100 μ M Vinblastine (Sigma) for 2 h. After incubation times, cells were washed, scraped and resuspended in sample buffer

containing 1% 2-mercaptoethanol and sonicated for 10 min at 4 °C. The samples were frozen until use. For western blots analysis, the protein extracts were subjected to electrophoresis in 12.5% SDS-PAGE gels, transferred to a nitrocellulose membrane and blocked. The nitrocellulose membrane was incubated overnight at 4 °C with rabbit anti-LC3 (1:300), washed and incubated with a secondary HRP-conjugated anti-rabbit antibody (Jackson ImmunoResearch Laboratories) at a 1:10 000 dilution. Equal proteins loading were confirmed using mouse anti-Actin antibody (1:10 000). The bands were visualized with the ECL reagent (GE Healthcare), and analyzed using ImageJ software.

Apoptosis determinations

Nuclear fragmentation detected with Hoechst 33258. HeLa cells were plated on coverslips distributed in 24-well plates and transfected with different plasmids. Transfected cells uninfected or infected with *Cb* for 24 h were treated with or without chloramphenicol (80 µg/ml) for 18 h. Cells were exposed to UV light for 15 min to induce apoptosis. Afterward, cells were washed with PBS, fresh infection media was added and the incubation was continued for additional 6 h at 37 °C. Next, cells were subjected to indirect immunofluorescence. The bacteria and apoptotic nuclei were stained with Hoechst 33258. Cells were analyzed by fluorescence microscopy using an inverted microscope (Nikon Eclipse 2000). The percentages of apoptotic cells were evaluated as the ratio between the number of apoptotic cells and the number of total cells.

Tunel assay. HeLa cells were plated on coverslips distributed in 24-well plates and transfected with different plasmids. Transfected cells were uninfected or infected with *Cb* for 24 h and treated with or without chloramphenicol (80 µg/ml) for 18 h. Cells were exposed to UV light for 15 min to induce apoptosis. Then, cells were washed with PBS, fresh infection media was added, and the incubation was continued for additional 6 h at 37 °C. Next, cells were fixed with 3% paraformaldehyde in PBS and subjected to indirect immunofluorescence to detect Beclin 1. Then, cells were re-permeabilized with 0.1% Triton X-100 in PBS and incubated with TUNEL reaction mixture according to the manufacturer's protocol (Promega). The bacteria and apoptotic nuclei were stained with Hoechst 33258. Cells were analyzed using fluorescence microscopy with a FV100 Olympus Confocal Microscope. The percentages of apoptotic cells were evaluated as the ratio between the number of apoptotic cells and the number of total cells.

Statistical analysis. The results are represented as the mean ± S.E.M. from at least three independent experiments. The comparisons were performed using ANOVA in conjunction with Tuckey's and Dunnett's tests. The significant differences were **P*<0.05; ***P*<0.01; and ****P*<0.001.

Acknowledgements. We are grateful to Dr. Luis Mayorga and Cecilia Lerena for critical reading of this paper. We also thank Alejandra Medero for excellent technical assistance with tissue culture, and Marcelo Furlán and Graciela Gutiérrez for technical assistance. This work was partly supported by grants from Agencia Nacional de Promoción Científica y Tecnológica (PICT2004 no. 20711 and PICT2005 no. 38420), CONICET (PIP no. 5943) and SECTyP (Universidad Nacional de Cuyo).

Conflict of interest

The authors declare no conflict of interest.

- Dunn Jr WA. Autophagy and related mechanisms of lysosome-mediated protein degradation. *Trends Cell Biol* 1994; 4: 139–143.
- Dunn Jr WA. Studies on the mechanisms of autophagy: formation of the autophagic vacuole. *J Cell Biol* 1990; 110: 1923–1933.
- Mizushima N. The pleiotropic role of autophagy: from protein metabolism to bactericide. *Cell Death Differ* 2005; 12 (Suppl 2): 1535–1541.
- Xie Z, Klionsky DJ. Autophagosome formation: core machinery and adaptations. *Nat Cell Biol* 2007; 9: 1102–1109.
- Cao Y, Klionsky DJ. Physiological functions of Atg6/Beclin 1: a unique autophagy-related protein. *Cell Res* 2007; 17: 839–849.
- Petiot A, Pattingre S, Arico S, Meley D, Codogno P. Diversity of signaling controls of macroautophagy in mammalian cells. *Cell Struct Funct* 2002; 27: 431–441.
- Petiot A, Ogier-Denis E, Blommaert EF, Meijer AJ, Codogno P. Distinct classes of phosphatidylinositol 3'-kinases are involved in signaling pathways that control macroautophagy in HT-29 cells. *J Biol Chem* 2000; 275: 992–998.

- Ohsumi Y. Molecular dissection of autophagy: two ubiquitin-like systems. *Nat Rev Mol Cell Biol* 2001; 2: 211–216.
- Mizushima N, Yamamoto A, Hatano M, Kobayashi Y, Kabeya Y, Suzuki K *et al.* Dissection of autophagosome formation using Apg5-deficient mouse embryonic stem cells. *J Cell Biol* 2001; 152: 657–668.
- Mizushima N, Ohsumi Y, Yoshimori T. Autophagosome formation in mammalian cells. *Cell Struct Funct* 2002; 27: 421–429.
- Tanida I, Ueno T, Kominami E. LC3 conjugation system in mammalian autophagy. *Int J Biochem Cell Biol* 2004; 36: 2503–2518.
- Kabeya Y, Mizushima N, Yamamoto A, Oshitani-Okamoto S, Ohsumi Y, Yoshimori T. LC3, GABARAP and GATE16 localize to autophagosomal membrane depending on form-II formation. *J Cell Sci* 2004; 117 (Pt 13): 2805–2812.
- Kabeya Y, Mizushima N, Ueno T, Yamamoto A, Kirisako T, Noda T *et al.* LC3, a mammalian homologue of yeast Apg8p, is localized in autophagosome membranes after processing. *EMBO J* 2000; 19: 5720–5728.
- Qu X, Yu J, Bhagat G, Furuya N, Hibshoosh H, Troxel A *et al.* Promotion of tumorigenesis by heterozygous disruption of the beclin 1 autophagy gene. *J Clin Invest* 2003; 112: 1809–1820.
- Yue Z, Jin S, Yang C, Levine AJ, Heintz N. Beclin 1, an autophagy gene essential for early embryonic development, is a haploinsufficient tumor suppressor. *Proc Natl Acad Sci USA* 2003; 100: 15077–15082.
- Aita VM, Liang XH, Murty VV, Pincus DL, Yu W, Cayanis E *et al.* Cloning and genomic organization of beclin 1, a candidate tumor suppressor gene on chromosome 17q21. *Genomics* 1999; 59: 59–65.
- Liang XH, Jackson S, Seaman M, Brown K, Kempkes B, Hibshoosh H *et al.* Induction of autophagy and inhibition of tumorigenesis by beclin 1. *Nature* 1999; 402: 672–676.
- Boya P, Gonzalez-Polo RA, Casares N, Perfettini JL, Dessen P, Larochette N *et al.* Inhibition of macroautophagy triggers apoptosis. *Mol Cell Biol* 2005; 25: 1025–1040.
- Maiuri MC, Le Toumelin G, Criollo A, Rain JC, Gautier F, Juin P *et al.* Functional and physical interaction between Bcl-X(L) and a BH3-like domain in Beclin-1. *EMBO J* 2007; 26: 2527–2539.
- Oberstein A, Jeffrey PD, Shi Y. Crystal structure of the Bcl-XL-Beclin 1 peptide complex: Beclin 1 is a novel BH3-only protein. *J Biol Chem* 2007; 282: 13123–13132.
- Pattingre S, Tassa A, Qu X, Garuti R, Liang XH, Mizushima N *et al.* Bcl-2 antiapoptotic proteins inhibit Beclin 1-dependent autophagy. *Cell* 2005; 122: 927–939.
- Dom BR, Dunn Jr WA, Progulsk-Fox A. Bacterial interactions with the autophagic pathway. *Cell Microbiol* 2002; 4: 1–10.
- Pizarro-Cerda J, Moreno E, Sanguedolce V, Mege JL, Gorvel JP. Virulent Brucella abortus prevents lysosome fusion and is distributed within autophagosome-like compartments. *Infect Immun* 1998; 66: 2387–2392.
- Amer AO, Swanson MS. Autophagy is an immediate macrophage response to Legionella pneumophila. *Cell Microbiol* 2005; 7: 765–778.
- Heinzen RA, Hackstadt T, Samuel JE. Developmental biology of Coxiella burnetii. *Trends Microbiol* 1999; 7: 149–154.
- McCaul TF, Williams JC. Developmental cycle of Coxiella burnetii: structure and morphogenesis of vegetative and sporogenic differentiations. *J Bacteriol* 1981; 147: 1063–1076.
- Sexton JA, Vogel JP. Type IVB secretion by intracellular pathogens. *Traffic* 2002; 3: 178–185.
- Beron W, Gutierrez MG, Rabinovitch M, Colombo MI. Coxiella burnetii localizes in a Rab7-labeled compartment with autophagic characteristics. *Infect Immun* 2002; 70: 5816–5821.
- Gutierrez MG, Vazquez CL, Munafó DB, Zoppino FC, Beron W, Rabinovitch M *et al.* Autophagy induction favours the generation and maturation of the Coxiella-replicative vacuoles. *Cell Microbiol* 2005; 7: 981–993.
- Romano PS, Gutierrez MG, Beron W, Rabinovitch M, Colombo MI. The autophagic pathway is actively modulated by phase II Coxiella burnetii to efficiently replicate in the host cell. *Cell Microbiol* 2007; 9: 891–909.
- Howe D, Melnicakova J, Barak I, Heinzen RA. Maturation of the Coxiella burnetii parasitophorous vacuole requires bacterial protein synthesis but not replication. *Cell Microbiol* 2003; 5: 469–480.
- Akporiaye ET, Rowatt JD, Aragon AA, Baca OG. Lysosomal response of a murine macrophage-like cell line persistently infected with Coxiella burnetii. *Infect Immun* 1983; 40: 1155–1162.
- Voth DE, Heinzen RA. Lounging in a lysosome: the intracellular lifestyle of Coxiella burnetii. *Cell Microbiol* 2007; 9: 829–840.
- Voth DE, Howe D, Heinzen RA. Coxiella burnetii inhibits apoptosis in human THP-1 cells and monkey primary alveolar macrophages. *Infect Immun* 2007; 75: 4263–4271.
- Luhmann A, Roy CR. Coxiella burnetii inhibits activation of host cell apoptosis through a mechanism that involves preventing cytochrome c release from mitochondria. *Infect Immun* 2007; 75: 5282–5289.
- Maiuri MC, Zalckvar E, Kimchi A, Kroemer G. Self-eating and self-killing: crosstalk between autophagy and apoptosis. *Nat Rev Mol Cell Biol* 2007; 8: 741–752.
- Levine B, Sinha S, Kroemer G. Bcl-2 family members: dual regulators of apoptosis and autophagy. *Autophagy* 2008; 4: 600–606.

38. Sanjuan MA, Dillon CP, Tait SW, Moshiah S, Dorsey F, Connell S *et al*. Toll-like receptor signalling in macrophages links the autophagy pathway to phagocytosis. *Nature* 2007; **450**: 1253–1257.
39. Brady NR, Hamacher-Brady A, Yuan H, Gottlieb RA. The autophagic response to nutrient deprivation in the h1-1 cardiac myocyte is modulated by Bcl-2 and sarco/endoplasmic reticulum calcium stores. *FEBS J* 2007; **274**: 3184–3197.
40. Dong F, Pirbhai M, Xiao Y, Zhong Y, Wu Y, Zhong G. Degradation of the proapoptotic proteins Bik, Puma, and Bim with Bcl-2 domain 3 homology in Chlamydia trachomatis-infected cells. *Infect Immun* 2005; **73**: 1861–1864.
41. Carmen JC, Hardi L, Sinai AP. Toxoplasma gondii inhibits ultraviolet light-induced apoptosis through multiple interactions with the mitochondrion-dependent programmed cell death pathway. *Cell Microbiol* 2006; **8**: 301–315.
42. Banga S, Gao P, Shen X, Fiscus V, Zong WX, Chen L *et al*. Legionella pneumophila inhibits macrophage apoptosis by targeting pro-death members of the Bcl2 protein family. *Proc Natl Acad Sci USA* 2007; **104**: 5121–5126.
43. Shimizu S, Kanaseki T, Mizushima N, Mizuta T, Arakawa-Kobayashi S, Thompson CB *et al*. Role of Bcl-2 family proteins in a non-apoptotic programmed cell death dependent on autophagy genes. *Nat Cell Biol* 2004; **6**: 1221–1228.
44. Wang J, Lian H, Zhao Y, Kaus MA, Spindel S. Vitamin D3 induces autophagy of human myeloid leukemia cells. *J Biol Chem* 2008; **283**: 25596–25605.
45. Swerdlow S, McColl K, Rong Y, Lam M, Gupta A, Distelhorst CW. Apoptosis inhibition by Bcl-2 gives way to autophagy in glucocorticoid-treated lymphocytes. *Autophagy* 2008; **4**: 612–620.
46. Ciechomska IA, Goemans GC, Skepper JN, Tolkovsky AM. Bcl-2 complexed with Beclin-1 maintains full anti-apoptotic function. *Oncogene* 2009; **28**: 2128–2141.
47. Voth DE, Heinzen RA. Sustained activation of Akt and Erk1/2 is required for Coxiella burnetii anti-apoptotic activity. *Infect Immun* 2009; **77**: 205–213.
48. Manning BD, Cantley LC. AKT/PKB signaling: navigating downstream. *Cell* 2007; **129**: 1261–1274.
49. Howe D, Barrows LF, Lindstrom NM, Heinzen RA. Nitric oxide inhibits Coxiella burnetii replication and parasitophorous vacuole maturation. *Infect Immun* 2002; **70**: 5140–5147.

Supplementary Information accompanies the paper on Cell Death and Differentiation website (<http://www.nature.com/cdd>)